

1 **Identification and characterization of bisbenzimidazole compounds that inhibit**
2 **human cytomegalovirus replication**

3
4 Nicole Falci Finardi¹ ¶, HyeonJun Kim^{2,3}, Lee Z Hernandez^{2,3,4}, Matthew RG
5 Russell⁵, Catherine M-K Ho¹, Vattipally B Sreenu⁶, Hannah A Wenham¹,
6 Andy Merritt⁷, & Blair L Strang^{1,8} ¶*

7
8 ¹Institute of Infection & Immunity, St George's, University of London, London,
9 United Kingdom

10 ²Department of Physics and Astronomy and ³Biochemistry and Molecular Biology
11 Program, University of Texas Rio Grande Valley, Edinburg, Texas, United States
12 of America

13 ⁴Department of Physics, Applied Physics and Astronomy, Rensselaer
14 Polytechnic Institute, Troy, New York, United States of America

15 ⁵The Francis Crick Institute, London, United Kingdom

16 ⁶MRC- University of Glasgow Centre for Virus Research, University of Glasgow,
17 Glasgow, United Kingdom

18 ⁷Centre for Therapeutic Discovery, LifeArc, Stevenage, United Kingdom

19 ⁸Department of Biological Chemistry & Molecular Pharmacology, Harvard Medical
20 School, Boston, Massachusetts, United States of America

21

22 *Corresponding author email: bstrang@sgul.ac.uk

23 ¶ These authors contributed equally to this work

24 **Abstract**

25

26 The shortcomings of current anti-human cytomegalovirus (HCMV) drugs
27 has stimulated a search for anti-HCMV compounds with novel targets. We
28 screened collections of bioactive compounds and identified a range of compounds
29 with the potential to inhibit HCMV replication. Of these compounds, we selected
30 bisbenzimidazole compound RO-90-7501 for further study. We generated analogues
31 of RO-90-7501 and found that one compound, MRT00210423, had increased anti-
32 HCMV activity compared to RO-90-7501. Using a combination of compound
33 analogues, microscopy and biochemical assays we found RO-90-7501 and
34 MRT00210423 interacted with DNA. In single molecule microscopy experiments
35 we found RO-90-7501, but not MRT00210423, was able to compact DNA,
36 suggesting that compaction of DNA was non-obligatory for anti-HCMV effects.
37 Using bioinformatics analysis, we found that there were many putative
38 bisbenzimidazole binding sites in the HCMV DNA genome. However, using western
39 blotting, quantitative PCR and electron microscopy, we found that at a
40 concentration able to inhibit HCMV replication our compounds had little or no effect
41 on production of certain HCMV proteins or DNA synthesis, but did have a notable
42 inhibitory effect on HCMV capsid production. We reasoned that these effects may
43 have involved binding of our compounds to the HCMV genome and/or host cell
44 chromatin. Therefore, our data expands our understanding of compounds with
45 anti-HCMV activity and suggests targeting of DNA with bisbenzimidazole compounds
46 may be a useful anti-HCMV strategy.

47 **Introduction**

48

49 Disease caused by human cytomegalovirus (HCMV) is wide ranging and
50 has significant social and economic impact (1). Currently, there is no widely
51 available vaccine against HCMV (1, 2). Plus, the use of first and second line anti-
52 viral drugs inhibiting the HCMV DNA polymerase (ganciclovir and foscarnet) have
53 a number of shortcomings, including the development of anti-viral resistance (3).

54 The identification of novel anti-HCMV drugs (4, 5) has focused on finding
55 compounds that inhibit the function of a limited number of HCMV proteins,
56 including the HCMV kinase UL97 and the HCMV DNA packaging complex proteins
57 (5, 6). However, like ganciclovir and foscarnet, novel anti-HCMV drugs targeting
58 UL97, or DNA packaging complex proteins, also have significant issues with the
59 development of anti-viral resistance (7-12) or are thought to have poor efficacy in
60 clinical trials (13, 14). To overcome the development of anti-viral resistance when
61 targeting proteins expressed by HCMV, there has been interest in inhibiting the
62 function of cellular proteins required for HCMV replication. The stability of the
63 cellular genome would limit the occurrence of mutations that would allow anti-viral
64 resistance to occur.

65 A number of cellular proteins required for HCMV replication have been
66 identified (15) and there have been efforts to identify compounds known to inhibit
67 the function of cellular proteins required for anti-HCMV replication (some examples
68 of which can be found in references (16-22)). However, none of the compounds
69 identified in the aforementioned works have progressed toward clinical

70 development due to a number of factors, for example polypharmacology of the
71 compounds identified.

72 Novel strategies for inhibition of HCMV replication need to be explored. To
73 this end, we decided to screen compounds with known bioactive activity for anti-
74 HCMV activity.

75

CONFIDENTIAL

76 **Materials and methods**

77

78 **Cells and viruses**

79 Human foreskin fibroblast (HFF) cells (clone Hs29) were obtained from
80 American Type Culture Collection no. CRL-1684 (ATCC, Manassas, VA). All cells
81 were maintained in complete media: Dulbeccos Modified Eagles Medium (DMEM)
82 containing 10% fetal bovine serum (FBS), plus penicillin and streptomycin (all
83 Gibco). HCMV strains AD169 and Merlin(R1111) were kindly provided by Don
84 Coen (Harvard Medical School) and Richard Stanton (Cardiff University),
85 respectively.

86

87 **Compounds collections**

88 Microsource-1 US Drug Collection (Discover Systems) contained
89 compounds that had reached clinical trial stage in the USA. LOPAC 1 (Sigma-
90 Aldrich) contained known pharmacologically active compounds. NIH Clinical
91 Collection (BioFocus) comprised the 2012 versions of compound collections NCC1
92 and NCC2, which contained compounds that had a history of use in clinical trials.
93 All compounds were resuspended in DMSO (stock solution concentrations for
94 each collection were 2 mg/mL, 10 mM and 10 mM, respectively.)

95

96 **High throughput screening of compounds**

97 We have previously described infection of HFF cells with HCMV strain
98 AD169 for high throughput screening, preparation of screening plates for high

99 throughput microscopy analysis, microscopy analysis of screening plates and
100 analysis of screening results in several works describing screening small
101 molecules and siRNA collections (20-23). The experimental methodology is
102 described in the results section. The final amount of each compound in the
103 screening assay was: Microsource – 200ng, LOPAC – 28 μ M, NIH – 28 μ M.

104 To assess the quality of data that could be returned from the screening
105 protocol, we calculated the Z'-factor (24, 25) derived from the positive (heparan
106 sulphate treated infected cells) and negative (DMSO treated infected cells) control
107 wells. The screening controls for one plate in the LOPAC collection returned Z'-
108 factors of less than 0.5. Thus, the data from that plate was discarded. All other
109 screening plates returned Z'-factors of greater than or equal to 0.5, indicating a
110 robust separation of difference in the data derived from positive and negative
111 controls.

113 **Compounds**

114 RO-90-7501 (2'-(4-Aminophenyl)-[2,5'-bi-1*H*-benzimidazol]-5-amine) was
115 purchased from Tocris. We synthesized MRT00210423, MRT00210424,
116 MRT00210425 MRT00210426 and MRT00210427 using the schemes shown in
117 Figure S1. All compounds were resuspended in DMSO.

118

119

120

121

122 **Viral yield reduction assays**

123 Assays were performed essentially as described in (26). HFF cells were
124 plated at 5×10^4 cells per well in 24-well plates. After overnight incubation, cells
125 were infected with HCMV at a multiplicity of infection (MOI) of 1. After virus
126 adsorption for 1 hour at 37°C, cells were washed and incubated with 0.5 ml of
127 media containing DMSO or compounds at a range of concentrations. Plates were
128 incubated for 4 days at 37°C. Titers were determined by serial dilution of viral
129 supernatant onto HFF monolayers which were covered in DMEM containing 5%
130 FBS, 0.6% methylcellulose and antibiotics. Cultures were incubated for 14 days,
131 cells were stained with crystal violet and plaques were counted. The final
132 concentration of DMSO in all samples was maintained at <1% (v/v). The EC50
133 value of data from this assay was calculated using GraphPad.

134

135 **MTT cytotoxicity assays**

136 Assays were performed essentially as described (26). In this colorimetric
137 assay the ability of cellular NAD(P)H-dependent cellular oxidoreductase enzymes
138 to reduce the tetrazolium dye 3-(4,5-dimethylthiazol-2-yl)-2,5-diphenyltetrazolium
139 bromide (MTT) to formazan was measured. HFF cells were seeded at 1×10^4 or
140 1×10^3 cells per well into 96-well plates. High concentrations of cells (1×10^4 per well)
141 should assess cell viability, whereas low concentrations of cells (1×10^3 per well)
142 should assess both cell viability and cell proliferation. After overnight incubation to

143 allow cell attachment, cells were treated for 96 hours with a range of
144 concentrations of compound, or the equivalent volume of DMSO. MTT assays
145 were then performed according to the manufacturer's instructions (GE Healthcare).
146 The final concentration of DMSO in all samples was maintained at <1% (v/v).

147

148 **Light microscopy**

149 HFF cells were seeded in 24 well tissue culture plates (5×10^4 cells/well).
150 Twenty four hours later, cells were treated with the concentrations of compound
151 inducted in the text or the equivalent volume of DMSO in complete media. After 1
152 hour incubation with compounds or DMSO at 37°C, cells were placed at room
153 temperature followed by incubation with ice cold methanol (30 mins). Cells were
154 washed with phosphate buffered saline and imaged using a Zeiss Axioplan 2
155 microscope.

156

157 **Agarose gel electrophoresis**

158 Plasmid pUC19 (a kind gift from Steve Goodbourn (St George's, University
159 of London), was linearized by digestion with enzyme EcoRI using the supplier's
160 (New England Biolabs) instructions. A 0.8% TAE agarose gel was prepared with
161 compound added to a concentration of 10 μ M and the linearized plasmid was
162 introduced into the gel via electrophoresis. Also introduced into the gel was a
163 ladder of DNA markers (N3232S, New England Biolabs). The gel was exposed to
164 UV light and images of the gel were captured using a Syngene camera apparatus.

165 **Analysis of putative binding sites in the HCMV genome**

166 The complete analysis pipeline along with the source code is available on
167 the GitHub page (<https://github.com/vbsreenu/find-motif>). Briefly, genome
168 sequences in fasta format and gene features in gff format were downloaded from
169 GenBank with the help of NCBI's eutils API (scripts are available on GitHub:
170 <https://github.com/vbsreenu/find-motif>). Using a custom FIND_MOTIF program,
171 nucleotide motifs were extracted from genome sequence files and their
172 corresponding gene features from gff file. The FIND_MOTIF program was
173 developed in C programming language using Karp-Robin string search algorithm
174 to find nucleotide motifs (kmers) in the genome sequence file. The locations of the
175 motifs were then compared with genome features table file using an AWK script to
176 find whether the motifs were part of any coding region. Final results were stored in
177 a specified output file.

178

179

180 **Dual labeling of Bacteriophage Lambda genomic DNA for single-molecule** 181 **microscopy**

182 Bacteriophage lambda genomic DNA (lambda DNA) with a digoxigenin
183 moiety at one termini (to label DNA with a quantum dot) and a biotin moiety at the
184 other termini (to tether the DNA onto the surface of a microfluidic flow cell through
185 biotin-neutraavidin interaction) was prepared as previously described elsewhere
186 (27). Briefly, lambda DNA had 12 nucleotide overhangs at both ends. Biotin-
187 labeled (5'- agg tcg ccg ccc/3'BioTEG/ -3') and digoxigenin (5'- ggg cgg cga cct

188 aaa aaa aaa aaa /3'Dig_N)-labeled oligos complementary to the overhangs were
189 annealed and ligated to lambda DNA. The ligation reaction mixture was run on a
190 0.4% agarose gel, allowing unconjugated excess oligos to be separated from
191 labeled DNA by electrophoresis. The DNA band corresponding to the biotin and
192 digoxigenin labeled lambda DNA was excised from the gel. The purified biotin and
193 digoxigenin labeled lambda DNA was recovered from the excised agarose gel in
194 a dialysis bag and concentrated using an ethanol precipitation of DNA procedure.

195

196 **Preparation of a flow cell for single-molecule microscopy flow-stretching** 197 **assays**

198 A microfluidic flow cell was assembled using a quartz top, a surface-
199 passivated cover glass (using polyethylene glycol), double-sided tape, and inlet
200 and outlet tubes as previously described elsewhere (27, 28). Approximately 4% of
201 the polyethylene glycol layer on the cover glass had biotin moieties onto which
202 were tethered the dual labeled lambda DNAs described above. To fix the dual
203 labeled lambda DNA to the glass cover, 0.25 mg/mL neutravidin was added to the
204 flow cell and incubated for at least 5 minutes. The excess neutravidin was removed
205 by flowing Qdot-labeling buffer (10mM Tris, pH 8.0, 150mM NaCl, 10mM MgCl₂,
206 0.2 mg/mL bovine serum albumin) into the flow cell. Then, the biotin and
207 digoxigenin labeled lambda DNA was flowed into the flow cell at a rate of 30
208 μ L/min. Excess dual labeled DNAs not joined to the cover glass surface were
209 removed by flowing in Qdot-labeling buffer. Quantum dots were affixed to DNA by
210 flowing 250 μ L of 750-fold diluted anti-digoxigenin-conjugated quantum dot 605

211 (Thermo Fisher Scientific S10469, anti-digoxigenin antibody: GeneTex
212 GTX73152) at a rate of 30 μ L/min. The flow cell was washed to remove the excess
213 quantum dots by flowing imaging buffer (20mM Tris, pH 7.5, 150mM NaCl, 2mM
214 $MgCl_2$, 1.2 mg/mL bovine serum albumin) into the flow cell at a rate of 50 μ L/min.

215

216 **Data capture and analysis in single-molecule DNA flow-stretching assays**

217 Compound was diluted in imaging buffer containing bovine serum albumin
218 at the concentrations mentioned in the text. Compound or DMSO were flowed into
219 the cell at a rate of 50 μ L/min. Quantum dots labeled on lambda DNA were imaged
220 under a total internal reflection fluorescence microscope with 532 nm laser
221 illumination. Movement of quantum dots (Lambda DNA compaction events) were
222 recorded using Micro-Manager software (29) and, subsequently, kymographs
223 were prepared using ImageJ (30).

224

225 **Western blotting**

226 HFF cells (5×10^4 cells/well) were infected with virus (MOI 1) and treated with
227 the concentrations of compounds indicated in the text or the equivalent volume of
228 DMSO. All samples were prepared for western blotting by washing cells once in
229 PBS, then suspending cells directly in 50 μ l 2x Laemmli buffer containing 5% β -
230 mercaptoethanol before incubating at 95°C for 5 mins. Western blotting of proteins
231 was carried out as described elsewhere (31), using antibodies recognizing IE1/2,
232 UL57, pp28, (all Virusys, 1:1000 dilution), UL86 (a kind gift from Wade Gibson
233 (Johns Hopkins School of Medicine) 1:1000 dilution) and β -actin (SIGMA, 1:5000

234 dilution). All primary antibodies were incubated overnight at 4°C and detected
235 using an anti-mouse- or anti-rabbit- horseradish peroxidase (HRP) conjugated
236 antibody (New England Biolabs). Chemiluminescence solution (GE Healthcare)
237 was used to detect secondary antibodies on film.

238

239 **Real time quantitative PCR analysis of viral DNA synthesis in HCMV infected** 240 **cells**

241 Preparation of samples for PCR and PCR analysis were conducted using
242 the methodology and reagents we have described elsewhere (23, 32, 33) to
243 calculate the number of copies of the viral gene *UL83* per copy of the cellular gene
244 *adipsin*. Statistical analysis was performed using Graphpad.

245

246 **Electron microscopy analysis of HCMV infected cells**

247 HCMV infected HFF cells were treated as outlined in the figure legend. To
248 prepare cells for analysis, cells were incubated for 1 h at room temperature in
249 fixative (1.5% glutaraldehyde and 4% paraformaldehyde in 0.1M sodium
250 cacodylate buffer [pH 7.4]). After fixation, cells were washed 3 x 15 mins in 0.1 M
251 sodium phosphate buffer (pH 7.4) and dehydrated in ethanol (50%, 70%, 90%, 15
252 mins wash each). Cells were then washed in 90% ethanol containing LR-White
253 embedding media (2 hours) and transferred to gelatin capsules (polymerization
254 55°C for 24 hours).

255 Eighty nm sections of each capsule were stained with lead citrate and
256 imaged in a 1400 FLASH transmission electron microscope (JEOL) at -2 µm

257 defocus with 2.8 nm pixels using 2x2 TEM Center montaging. Montages were then
258 converted to mrc format and contrast adjusted, before outputting as a 1:1 tif series
259 with the 'movie' function, using the tif2mrc and 3dmod packages of IMOD (34).
260

CONFIDENTIAL

261 **Results**

262

263 **Screening of bioactive compound collections**

264 We have previously employed an automated high throughput screening
265 methodology to identify compounds and siRNAs with potential anti-HCMV activity
266 (20-23). We used this methodology to screen collections of bioactive compounds
267 in the NIH Clinical, Microsource, and LOPAC collections for potential anti-HCMV
268 activity. Briefly, cells infected with the high passage HCMV strain AD169 (35) were
269 treated with compounds from each collection. Two factors were then assayed
270 using automated microscopy; the number of cells in each well and the number of
271 cells expressing the HCMV antigen pp28. pp28 is essential for HCMV replication
272 (36) and its expression late in HCMV replication is dependent on viral DNA
273 synthesis (37). Therefore, our screen had the potential to identify compounds able
274 to inhibit several stages of HCMV replication, including viral DNA synthesis. Those
275 compounds that produced a decrease in the number of cells in the assay by 50%
276 or greater were judged to be cytotoxic to HCMV infected cells (Tables S1-S3) and
277 were not studied further. Remaining data from the screen were then converted to
278 a z-score (the number of standard deviations from the mean of the data (24, 25))
279 to show an increase or decrease in the number of cells expressing pp28 (positive
280 or negative z-score, respectively) (Fig. 1 and Tables S4-S6).

281 We investigated if our screening results were consistent with the activity of
282 known anti-viral compounds and data previously reported using these compound
283 collections. We noted that one antiviral compound with known anti-HCMV activity,

284 PMEG (38), was assigned a negative z-score (-5.4 (Fig.1 and Table S6)), while an
285 antiviral compound known to have poor anti-HCMV activity, valaciclovir (39), was
286 assigned a z-score close to zero (0.4, (Fig. 1 and Table S4)). Therefore, our
287 screening data were consistent with the known anti-HCMV activity of at least two
288 compounds.

289 To our knowledge, the NIH Clinical Collection used here has not been
290 previously used to identify compounds with anti-HCMV activity. The Microsource
291 collection has been used in screening experiments to identify compounds with anti-
292 HCMV activity (16-18). However, these screens had different parameters to our
293 own (inhibition of ectopic GFP expression controlled by viral protein IE2 (16),
294 inhibition of IE2-YFP fusion protein expression from a recombinant HCMV virus
295 (17) and inhibition of fusion protein pp28-GFP expression from a recombinant
296 HCMV virus (18)) and, therefore, reported considerably different results. Screening
297 of the LOPAC collection for anti-HCMV activity using an assay different to our own
298 has been reported (19), but the screening methodology and the full list of
299 compounds with anti-HCMV activity found in the aforementioned screen has not
300 been reported (19). Therefore, it was not possible to compare our data with the
301 previously reported screen of the LOPAC collection.

302 We also considered if it were possible that some compounds were routinely
303 identified in a range of screens due to an unappreciated non-specific effect of the
304 compound. All three compound collections examined here have been used in a
305 range of screens, some mentioned above. To our knowledge, no other screening
306 experiment has reported the same findings as our screens. Therefore, the

307 compounds we identified in our screen may have had a specific anti-HCMV activity
308 and were unlikely to be identified due an unappreciated non-specific activity of the
309 compound.

310 The compounds assigned low z-scores (less than -2.0) in each collection
311 were examined further (Table 1). A wide range of compounds were found to inhibit
312 the expression of pp28 in our assay. Expression of pp28 is dependent on viral DNA
313 synthesis (37), which was consistent with compounds known to inhibit viral DNA
314 synthesis (PMEG) being assigned the lowest z-scores (Table 1). However, it was
315 unclear or unknown how a number of other compounds assigned low z-scores
316 (including Aurintricarboxylic acid, Floxuridine, Fludarabine or Hexachlorophene
317 (Table 1)) affected pp28 expression.

318 We then decided to choose a compound in Table 1 for further investigation.
319 We sought a compound that had a low z-score, had not previously been reported
320 to inhibit HCMV, may have had a target other than a viral or cellular protein and
321 could be amenable to modification. Based on these criteria, we chose to
322 investigate how RO-90-7501 (Fig. 1) might inhibit HCMV replication.

323 To our knowledge, there were no previous reports that RO-90-7501 could
324 inhibit HCMV replication. RO-90-7501 is a bisbenzimidazole compound and
325 structurally similar to other well-known bisbenzimidazole compounds that bind DNA,
326 such as the so-called “Hoechst dyes”, which bind in the minor groove of the DNA
327 helix via interactions with adenine-thymine base pairs (40) and fluoresce upon
328 exposure to ultraviolet (UV) light. A comparison of RO-90-7501 structure with the
329 structure of a well characterized Hoechst dye, Hoechst 33258, is shown in Figure

330 2. Also indicated in Figure 2 is the mechanism by which Hoechst 33258 binds to
331 DNA, principally through hydrogen bonds between amine groups in the Hoechst
332 33258 compound and groups within purine bases of the minor groove of DNA (40)
333 (red dotted lines, Fig. 2A) (40). As RO-90-7501 had the essential structure required
334 for DNA binding (40), we hypothesized that RO-90-7501 could interact with DNA
335 using the same mechanism as Hoechst 33258 (red dotted lines, Fig. 2B). To our
336 knowledge, there were no previous reports of HCMV replication inhibition by
337 bisbenzimidazole compounds or any other compound known to bind to the minor
338 groove of the DNA helix.

339 Before continuing further, we were concerned that bisbenzimidazole
340 compounds may have off target effects that affect cell viability in cell culture
341 experiments or *in vivo*, likely due to their ability to bind DNA. However, it had been
342 reported that Hoechst 33342 could inhibit poxvirus replication in cell culture
343 experiments with no obvious cellular toxicity (41). Plus, Hoechst 33342 has been
344 administered to mice with no obvious adverse effects (42) and the bisbenzimidazole
345 compound Pibenzimidazole has been administered to humans without obvious adverse
346 effects (43). Therefore, we speculated that RO-90-7501 and similar compounds
347 may not have off target effects that would obviously limit their use in cell culture or
348 *in vivo*.

349

350 **Identification of RO-90-7501 analogues anti-HCMV activity**

351 Modification of compound structure can often reveal novel compounds with
352 enhanced anti-viral activity. Therefore, to find novel compounds with anti-HCMV

353 activity we generated compounds structurally related to RO-90-7501 (Fig 3). As
354 DNA binding is likely to be essential for the anti-viral activity of RO-90-7501, we
355 decided that any compounds we generated must contain the amine groups within
356 RO-90-7501 that are likely to be required for DNA binding (highlighted in red, Fig.
357 3). It was unknown what, if any, effect the amine groups at the termini of RO-90-
358 7501 had on anti-HCMV activity (highlighted in green, Fig. 3). Therefore, we
359 focused on modifying the termini of RO-90-7501. We generated compounds that
360 did not possess either of the terminal amine groups (MRT00210425 and
361 MRT00210424) and a compound that had neither of the terminal amine groups
362 (MRT00210423) (Fig. 3).

363 We compared the anti-viral activity of these compounds to that of RO-90-
364 7501 and DMSO (Fig. 3). MRT00210425, MRT00210424 and MRT00210423 all
365 had anti-HCMV activity greater than that of RO-90-7501. Loss of either terminal
366 amino group of RO-90-7501 (MRT00210425 and MRT00210424) had a
367 moderately greater anti-viral effect compared to RO-90-7501, whereas loss of both
368 terminal amino groups (MRT00210423) showed the greatest anti-viral effect
369 compared to RO-90-7501. We decided to focus our efforts on studying the anti-
370 viral effects of MRT00210423 compared to RO-90-7501.

371

372 **Investigation of RO-90-7501 and MRT00210423 anti-HCMV activity**

373 To confirm that RO-90-7501 and MRT00210423 could inhibit HCMV
374 replication, a virus yield reduction assay was used to compare the production of
375 HCMV strain AD169 in the presence of increasing concentrations of RO-90-7501,

376 MRT00210423 or DMSO (Fig. 4A). We found a dose-dependent decrease in
377 HCMV production in the presence of both RO-90-7501 and MRT00210423,
378 indicating that both compounds were able to inhibit AD169 replication. The 50%
379 effective concentration (EC₅₀) values of RO-90-7501 and MRT00210423 were
380 calculated as 1.2 μ M and 0.3 μ M respectively. Consistent with the data shown in
381 Figure 3, the EC₅₀ value of MRT00210423 was greater than that of RO-90-7501.
382 We found similar results when we assayed the ability of RO-90-7501 to inhibit
383 replication of the low passage HCMV strain Merlin (Fig. 4B), whose genetic content
384 was similar to wild type strains of HCMV (35) (EC₅₀ of 2.6 μ M and 0.5 μ M for RO-
385 90-7501 and MRT00210423, respectively). Therefore, RO-90-7501 and
386 MRT00210423 could inhibit HCMV replication and could do so EC₅₀
387 concentrations similar to those reported for the current frontline anti-HCMV drug
388 ganciclovir (26, 44).

389 We then used an MTT assay to assess the viability of a high concentration
390 of uninfected cells treated with increasing concentrations of DMSO or RO-90-7501
391 (Fig. 4C). The 50% cellular toxicity concentration (CC₅₀) of both compounds was
392 in excess of 10 μ M, considerably greater than the EC₅₀ values observed in Fig.
393 4A. We also performed this assay with a low concentration of uninfected cells to
394 assess both cell viability and proliferation (Fig. 4D). The CC₅₀ concentration of
395 both compounds was in excess of 10 μ M. Therefore, treatment of cells with RO-
396 90-7501 or MRT00210423 had no obvious toxic effect in either assay and the
397 inhibition of virus replication observed in our virus yield reduction assays (Figs. 4A

398 and 4B) was unlikely to be due to toxic effects of either RO-90-7501 or
399 MRT00210423.

400

401 **Investigation of compound association with DNA**

402 To confirm that RO-90-7501 and MRT00210423 could associate with DNA,
403 we used light microscopy to understand if, like Hoechst compounds, RO-90-7501
404 and MRT00210423 could associate with host cell chromatin in uninfected cells.
405 HFF cells were treated with either RO-90-7501, MRT00210423 or DMSO. Upon
406 exposure to UV light, host cell chromatin could be visualized in cells treated with
407 both RO-90-7501 and MRT00210423 (Fig 5), suggesting that RO-90-7501 was
408 associated with host cell chromatin. We noted that visualization of chromatin in
409 cells treated with MRT00210423 was not as obvious as those cells treated with
410 RO-90-7501. However, we hypothesized that may have been due to differences in
411 fluorescence emission of RO-90-7501 and MRT00210423 or a difference in the
412 association of the compounds with chromatin. Treatment of cells with DMSO did
413 not result in the ability to visualize host cell chromatin in cells (Fig 5).

414 To confirm that our compounds interacted with DNA in the cell and not
415 another factor in the cell nuclei, we also asked if RO-90-7501 and MRT00210423
416 could associate with DNA outside of the cell. We have been unable to separate
417 HCMV DNA from cellular DNA in infected cell lysate or recover high concentrations
418 of intact HCMV genomes from preparations of HCMV virions (both data not
419 shown). Moreover, the size (over 230 kbp) and complexity of the HCMV genome
420 meant that HCMV genomes could not be easily manipulated in biochemical

421 assays. Therefore, for convenience, we assayed the ability of RO-90-7501 and
422 MRT00210423 to interact with linear plasmid DNA (Fig 6).

423 Biochemical studies of Hoechst 33258 interaction with DNA have identified
424 canonical DNA sequences to which bisbenzimidazole compounds are likely to
425 preferentially bind (40, 45). Further analysis of Hoechst 33258 binding to DNA
426 revealed that bisbenzimidazole compounds are likely to have different affinities for
427 these canonical DNA binding sites in cells (46). In order of greatest to lowest
428 affinity, bisbenzimidazole compounds are likely to bind to the canonical DNA
429 sequences: AAATT, ATTTT, AATAA, TATA, TTAATG, GTTTAT, TTTCT (46). To
430 test compound binding to DNA we used a plasmid (pUC19) that contained several
431 of the aforementioned sequences (Fig. 6A). We noted that these sequences are
432 present in high quantity in the sequence of the HCMV AD169 (Fig. 6B and listed
433 in Table S7). Also, the HCMV Merlin genome had a near identical number of each
434 putative binding site in its genome, compared to the AD169 genome (listed in Table
435 S8).

436 Linear plasmid DNA was introduced into an agarose gels containing either
437 RO-90-7501 or MRT00210423 using electrophoresis (Figs. 6C and 6D,
438 respectively). Upon exposure of the gel to UV light, a DNA band corresponding to
439 the expected molecular weight of the linear plasmid DNA was observed in both
440 experiments, suggesting that RO-90-7501 and MRT00210423 were associated
441 with plasmid DNA within the agarose gel. Again, we noted that visualization of DNA
442 in the presence of MRT00210423 was less obvious than in the experiment using
443 RO-90-7501. Incorporation of a volume of DMSO equivalent to that used in the

444 aforementioned experiment into agarose gels did not result in the visualization of
445 any DNA species (data not shown). Together, the data shown in Figs 5 and 6
446 confirmed that RO-90-7501 and MRT00210423 could associate with DNA.

447 To investigate the relationship between the ability of our compounds to bind
448 DNA and anti-HCMV effects, we generated two further compounds,
449 MRT00210426 and MRT00210427, which lacked either of the amine groups that
450 were likely required for binding of bisbenzimidazole compounds to DNA (40) (Fig 7, the
451 methyl groups substituted for amine groups highlighted in red in MRT00210426
452 and MRT00210427) and studied the ability of these compounds to inhibit HCMV
453 replication in virus replication assays (Fig 7). Compared to treatment of cells with
454 DMSO, we found that neither MRT00210426 nor MRT00210427 had any obvious
455 anti-HCMV effect, whereas MRT00210423 demonstrated an anti-HCMV effect
456 similar to that shown in Fig 3. This indicated that association of bisbenzimidazole
457 compounds with DNA was necessary for anti-HCMV activity.

458 To confirm the relationship between anti-HCMV activity and DNA
459 association of the aforementioned compounds we then tested the ability of
460 compounds to associate with DNA in agarose gels. A DNA molecular weight
461 marker was introduced into an agarose gels containing compounds indicated in
462 Fig 7 using electrophoresis (Fig. S3). Gels were then photographed upon exposure
463 to UV light, then washed in the UV light sensitive DNA stain SYBR Green and
464 again exposed to UV light and photographed. We found that DNA could be
465 observed in gel containing MRT00210423 upon initial exposure to UV light.
466 However, DNA could only be visualized in gels containing MRT00210426 or

467 MRT00210427 only after the gels were washed with the DNA stain SYBR Green.
468 This data suggested that MRT00210423 was associated with DNA in the agarose
469 gel, but MRT00210426 and MRT00210427 were not. Therefore, there was a
470 relationship between the ability of compounds to associate with DNA and anti-
471 HCMV effects. Furthermore, the binding of our compounds to host cell chromatin
472 (Fig. 5) and presence of putative bisbenzimidazole compound binding sites in the
473 HCMV genome (Fig. 6), suggested that our compounds may have bound to both
474 host cell chromatin and the HCMV genome in infected cells.

475

476

477 **Analysis of bisbenzimidazole action on DNA using single molecule microscopy**

478 We then attempted to understand what effect RO-90-7501 and
479 MRT00210423 might have on DNA in HCMV infected cells. It has been reported
480 that binding of bisbenzimidazole compounds to DNA can result in compaction of DNA
481 via condensation of the DNA helix (47), which could inhibit any number of biological
482 processes. We, therefore, used a single molecule flow-stretching technique to
483 analyze compaction of a DNA substrate in the presence of our bisbenzimidazole
484 compounds. In this assay a bacteriophage lambda genome (which contains 479
485 bisbenzimidazole binding sites) labeled with a quantum dot was placed within a
486 microfluidic flow cell into which buffer could flow. Using total internal reflection
487 fluorescence microscopy, the positions of a quantum dot was tracked in real-time
488 while the DNA was stretched by buffer flow. Quantum dot movement in the

489 presence of flow away or towards the tether could be interpreted to understand
490 elongation or compaction of the bacteriophage DNA, respectively (Fig. 8A).

491 We conducted a series of preliminary experiments in which increasing
492 concentrations of RO-90-7501 or MRT00210423 were flowed into a microfluidic
493 flow cell. We found that increasing concentrations of RO-90-7501 appeared to
494 quench emission from the quantum dots used. The same was found in the
495 presence of MRT00210423, albeit to what appeared to be a lesser extent.
496 Therefore, we assayed quantum dot movement at minimum concentration of RO-
497 90-7501 in which the quantum dots could be readily visualized while any change
498 in quantum dot movement was observed. Therefore, we flowed the volume of
499 DMSO equivalent to 75 μ M of either compound resuspended in DMSO into a flow
500 cell and found that the quantum dot visualized did not obviously move in the buffer
501 flow (Fig. 8B). However, when a concentration of 75 μ M RO-90-7501 was then
502 flowed into a flow cell emission from the quantum dot decreased over time and the
503 quantum dot moved, against the direction of buffer flow (Fig. 8C). However, when
504 75 μ M of MRT00210423 added to a flow cell there was no obvious movement of
505 the quantum dot in the presence of MRT00210423 (Fig. 8D). To ensure that the
506 lack of MRT00210423 compaction in this assay was not due to a concentration
507 dependent effect, we repeated the assay adding increasing concentrations of
508 MRT00201423 up to 1mM. However, we observed no compaction of DNA in the
509 presence of MRT00210423 at any of the compound concentrations tested (data
510 not shown).

511 Therefore, RO-90-7501 was able to compact DNA in this assay, whereas
512 MRT00210423 did not. This inferred that compaction of DNA in HCMV infected
513 cells was not obligatory for anti-HCMV effects and binding of compounds to DNA
514 alone was sufficient for our compounds to exert anti-HCMV effects.

515

516 **Investigation of HCMV replication in HCMV infected cells treated with** 517 **bisbenzimidazole compounds**

518 We then sought to understand how RO-90-7501 and MRT00210423
519 inhibited HCMV replication in infected cells. First, we investigated HCMV protein
520 production to understand at what point in HCMV replication our compounds acted.
521 A hallmark of HCMV replication is the production of proteins via a transcriptional
522 cascade of immediate-early, early and late transcription. Using western blotting,
523 we assayed the production of proteins representative of all three classes of viral
524 transcription (HCMV transcriptional transactivators IE1/IE2 representing proteins
525 produced via immediate early transcription, HCMV DNA binding protein UL57
526 representing proteins produced via early transcription, HCMV virion protein pp28
527 (tegument protein) and UL86 (major capsid protein) representing proteins
528 produced via late transcription) in the presence of either DMSO, RO-90-7501 or
529 MRT00210423 (Fig 9A). We found no obvious differences in the production of any
530 viral protein in the presence of 1 μ M RO-90-7501 or MRT00210423, compared to
531 viral protein production in the presence of DMSO. However, compared to viral
532 protein production in the presence of DMSO, there was a decrease in expression

533 of some viral proteins in the presence of 10 μ M RO-90-7501 and/or
534 MRT00210423.

535 We then assayed synthesis of HCMV DNA using a quantitative PCR
536 methodology (Fig. 9B). We assayed the number of viral DNA sequences compared
537 to the number of a cellular DNA sequence that could be found in HCMV infected
538 cells treated with either DMSO, RO-90-7501 or MRT00210423 (1 μ M or 10 μ M) at
539 immediate early (24 hours post infection) and late (96 hours post infection) time
540 points. Compared to viral DNA synthesis in the presence of DMSO, we found that
541 the presence of 1 μ M RO-90-7501 or MRT00210423 had little effect on viral DNA
542 synthesis, whereas the presence of 10 μ M RO-90-7501 or MRT00210423 had a
543 greater effect on viral DNA synthesis (Fig. 9B).

544 Therefore, the presence of 10 μ M RO-90-7501 or MRT00210423 was
545 sufficient to inhibit HCMV replication and HCMV protein production and DNA
546 synthesis (Figs. 4 and 9). However, the presence of 1 μ M RO-90-7501 or
547 MRT00210423 was sufficient to inhibit HCMV replication (Fig. 4), but was not
548 sufficient to obviously inhibit either viral protein production or viral DNA synthesis
549 (Fig. 9). Therefore, we speculated that there was a mechanism by which our
550 compounds inhibited HCMV replication that did not involve inhibition of HCMV
551 protein production or DNA synthesis. Packaging of nascent viral DNA into capsids
552 in the nucleus is essential for HCMV replication. We hypothesized that our
553 compounds may have interacted with newly synthesized HCMV DNA in the
554 nucleus and prevented HCMV DNA packaging into capsids. To investigate this,
555 we use electron microscopy of cells infected with HCMV in the presence of either

556 DMSO or 1 μ M or 10 μ M of our compounds. We counted the number of each of the
557 three capsid forms that can be found in HCMV infected nuclei (A capsids,
558 nonproductive forms thought to result from failed packaging of viral genomes; B
559 capsids, productive intermediates that contain a scaffolding protein; and C capsids,
560 assembled forms in which the scaffolding protein has been removed and replaced
561 with viral DNA) under each condition (Fig. 10). We anticipated that the presence
562 of our compounds might alter the ratio of B (empty) to C (DNA containing) capsids
563 found in infected nuclei, indicating a defect in genome packaging into capsids.
564 Surprisingly, while we observed large numbers of B capsids and smaller numbers
565 of A and C capsids in the presence of DMSO, we found little or no of any capsid
566 type in cells treated with either compound. Therefore, in the presence of 1 μ M of
567 our compounds inhibition of HCMV replication was associated with lack of HCMV
568 capsid production (Fig. 10), not inhibition of production of HCMV proteins analyzed
569 (including the major capsid protein UL86, Fig. 9A) or inhibition of viral DNA
570 synthesis (Fig. 9B). However in the presence of 10 μ M of our compounds, inhibition
571 of HCMV capsid production (Fig. 10) may have contributed to inhibition of HCMV
572 replication and was associated with inhibition of production of HCMV proteins
573 analyzed (including the major capsid protein UL86, Fig. 9A) and viral DNA
574 synthesis (Fig. 9B).

575 **Discussion**

576

577 We sought to increase the number of compounds available for inhibition of
578 HCMV replication by screening collections of bioactive compounds. Our screening
579 experiments identified a number of compounds not previously reported to inhibit
580 HCMV replication. We chose to study RO-90-7501, whose mechanism of action
581 was likely to be different from known anti-HCMV compounds. A key step in our
582 studies was to discover an analogue of RO-90-7501, MRT00210423, which we
583 found had greater anti-HCMV activity than RO-90-7501. We found that both RO-
584 90-7501 and MRT00210423 had efficient anti-HCMV activity, with no obvious
585 cellular toxicity, and that the anti-viral activity of the compounds was likely due to
586 their ability to interact with DNA. Interestingly, we found that RO-90-7501 and
587 MRT00210423 had different effects on DNA. Surprisingly, we observed an
588 association between the presence of compounds in infected cells and inhibition of
589 HCMV capsid production.

590 We considered why MRT00210423 had greater anti-HCMV activity than
591 RO-90-7501. Based upon an atomic structure of Hoechst 33258 binding to DNA,
592 we reasoned it was possible that MRT00210423 may have had a greater ability to
593 access the minor groove of DNA compared to RO-90-7501. The fit of Hoechst
594 33258 into the minor groove of the DNA was reported to be very close-fitting, with
595 Hoechst 33358 occupying the entire volume of the DNA minor groove (40). Binding
596 of Hoechst 33358 to DNA (40) involved a twist in the Hoechst 33358 structure and
597 arrangement of groups that comprise Hoechst 33358 was not co-planar.

598 Specifically, there was a small angle between the phenoic ring and the first
599 benzimidazole group and a much larger angle between the two consecutive
600 benzimidazole groups of the compound. The piperazine group was almost co-
601 planar with the neighboring benzimidazole group. Together, these data inferred
602 that Hoechst 33258 had to be fitted into the minor groove of DNA (40). Therefore,
603 we propose that removal of the terminal amine groups from RO-90-7501 allowed
604 a greater flexibility between the groups that comprise MRT00210423 and allowed
605 a more efficient fit of MRT00210423 into the minor DNA groove and, thus, easier
606 binding to DNA of MRT00210423 compared to RO-90-7501.

607 It was also possible that there were differences in metabolism of RO-90-
608 7501 and MRT00210423 within the cell that resulted in differences in anti-HCMV
609 activity between the two compounds. However, the structure of the two compounds
610 was similar. Therefore, it was not obvious what these differences in metabolism
611 might have been.

612 At a low concentration of our compounds we observed an association
613 between inhibition of HCMV replication and a lack of HCMV capsid production.
614 Presently, it is unknown what molecular mechanisms our compounds use to
615 prevent HCMV capsid production. Indeed, it is unclear or unknown how many
616 aspects of capsid formation take place, including what viral and cellular factors are
617 required for capsid formation and how these factors are localized and organized in
618 infected cell nuclei. It is possible that our compounds had effects on one or several
619 viral and cellular factors required for capsid formation. Furthermore, at a high
620 concentration of our compounds we also found inhibition of HCMV capsid

621 production. However, this could have been linked to defects we observed in HCMV
622 protein production and viral DNA synthesis in the presence of a high concentration
623 of our compounds. Presently, it is unknown if at a high concentration our
624 compounds act on gene expression or protein production of the viral factors
625 assayed in our experiments. That said, as we see efficient inhibition of HCMV
626 replication at a low concentration of our compounds, investigation of our
627 compounds at a high concentration is not a priority and future work should focus
628 on the surprising observation that links inhibition of HCMV replication with lack of
629 capsid production.

630 We hypothesized that our compounds would interact with HCMV DNA.
631 However, at a low concentration of our compounds we observed little or no defect
632 in HCMV DNA synthesis or production of those HCMV proteins analyzed. This
633 might suggest that our compounds did not act directly on HCMV DNA, but we
634 cannot exclude the possibility that compound binding to the viral genome affected
635 production of capsids via an as yet unknown mechanism. Interestingly, we have
636 found obvious interaction of both compounds with chromatin in uninfected cells.
637 Therefore, it was possible that binding of our compounds to cellular chromatin was
638 required for anti-HCMV effects. As production of those HCMV proteins analyzed
639 and DNA synthesis were not obviously compromised by our compounds, it is
640 unlikely that the interaction of our compounds with chromatin affected the
641 formation of nuclear HCMV replication compartments, within which HCMV DNA
642 synthesis occurs (48). Rather, we propose that binding of our compounds to
643 chromatin may have affected the production of one or many cellular factors

644 required for HCMV replication. Of course, it is possible that the anti-HCMV effects
645 of our compounds were due to compound binding to both viral DNA and chromatin.
646 We considered if a mechanism other than compound binding to DNA was
647 responsible for anti-HCMV effects. It should be noted that RO-90-7501 has been
648 reported to enhance transcription from the β -interferon promoter upon induction of
649 transcription using poly I:C (49). However, we found no evidence for the ability of
650 RO-90-7501 to enhance β -interferon production in HCMV infected cells (data not
651 shown) and the aforementioned work does not investigate what, if any, effects
652 interaction of RO-90-7501 with chromatin had on enhancing transcription from the
653 β -interferon promoter (49).

654 It is also interesting to consider the mechanistic details of how compound
655 binding to DNA resulted in anti-HCMV effects. We hypothesized that, like other
656 bisbenzimidazole compounds (47), binding of our compounds to DNA would result in
657 DNA compaction. DNA compaction could have multiple effects on DNA function.
658 However, we found compaction of DNA in the presence of RO-90-7501, but not
659 MRT00210423. Therefore, compaction of DNA for anti-HCMV effects was non-
660 obligatory and binding of compounds to DNA alone may have been sufficient for
661 anti-HCMV effects.

662 That said, RO-90-7501 and MRT00210423 could be useful tools in
663 biochemical studies of DNA compaction and its biological effects. It is possible that
664 DNA compaction by RO-90-7501 resulted in the formation of non-specific
665 structures in DNA and/or loop formation by bridging two different segments of a
666 DNA. Looping of DNA was consistent with the relatively long distance travelled by

667 DNA in our single molecule DNA stretching experiments in the presence of RO-
668 90-7501. The underlying mechanisms of DNA looping are largely unknown, but
669 important for essential biological processes. Comparing how our compounds bind
670 to DNA and how they have different effects could further our understanding of DNA
671 function in the cell.

672 For future development of compounds for clinical use it may be necessary
673 to find compounds related to RO-90-7501 and MRT00210423 that bind
674 preferentially to HCMV genomes compared to host cell chromatin. Bisbenzimidazole
675 compounds are amenable to a range of medicinal chemistry approaches (for
676 example see references (50-55)). These could lead to identification of analogues
677 of our compounds that preferentially bind HCMV genomes or the conjugation of
678 our compounds to DNA-binding proteins to target the compound to HCMV DNA.

679 That said, several factors support further development of RO-90-7501 or
680 MRT00210423 as anti-HCMV compounds. Current anti-HCMV therapy can be
681 limited by drug resistance (7-12). As yet, we have not been able to generate HCMV
682 viruses resistant to either RO-90-7501 or MRT00210423 (data not shown). Plus,
683 as mentioned above, it has been reported that administration of bisbenzimidazole
684 compounds has had no serious adverse effects in murine model experiments and
685 clinical trials in humans (42, 43). Finally, RO-90-7501 and MRT00210423 or
686 related compounds could have broad anti-viral activity, as it has been
687 demonstrated that bisbenzimidazole compounds have anti-viral activity against
688 poxviruses (41) and RO-90-7501 can inhibit replication of vesicular stomatitis virus
689 (49), a model virus for many important Rhabdoviruses affecting human health.

690

691 **AUTHOR CONTRIBUTIONS**

692

693 NFF: Investigation, Methodology, Formal Analysis, Writing-Review and Editing.

694 HJK: Investigation, Methodology, Formal Analysis. LZH: Investigation. MRGR:

695 Investigation, Methodology. CM-KH: Investigation, Methodology. VBS:

696 Investigation, Methodology. HAW: Methodology. AM: Conceptualization,

697 Methodology, Formal Analysis, Data Curation Resources, Supervision, Funding.

698 BLS: Conceptualization, Investigation, Methodology, Formal Analysis, Data

699 Curation, Resources, Writing-Original Draft Preparation, Writing-Review and

700 Editing, Supervision, Project Administration, Funding.

701

702 **CONFLICTS OF INTEREST**

703

704 The authors declare there are no conflicts of interest.

705

706 **FUNDING INFORMATION**

707

708

709 This work was supported by New Investigator funds from St George's, University

710 of London, St George's Impact & Innovation Awards (2014 and 2018), a

711 PARK/WestFocus Award, MRC Industrial CASE studentship MR/M016226/1

712 (all to BLS), plus the University of Texas Rio Grande Valley Start-up Grant and
713 the University of Texas System's Rising STARS Award (both to HJK). We are
714 grateful to Don Coen (Harvard Medical School) for his support of BLS during the
715 screening experiments featured here via grants awarded to DC from the National
716 Institutes of Health (R01 AI019838 and R01 AI026077).

717

718 **ACKNOWLEDGMENTS**

719

720 We are grateful to Don Coen for his encouragement during this study and
721 his support of BLS during the screening experiments. We also acknowledge Don
722 Coen, Steve Goodbourn, Richard Stanton and Wade Gibson and for kindly
723 providing reagents. For assistance with light and electron microscopy we thank
724 Greg Perry and all other members of the SGUL Image Resource Facility. Thanks,
725 also, to Lucy Collinson (Science Technology Platform, Francis Crick Institute) for
726 assistance electron microscopy. We thank Steve Goodbourn and Jason Mercer
727 for valuable discussions. Special thanks go to all members of Institute of Chemistry
728 and Chemical Biology-Longwood for their assistance in all aspects of the
729 compound screening process.

730

731

732 **Figure Legends**

733

734 **Fig 1. Compounds assigned z-scores.** The ability of compounds within the NIH
735 Clinical, Microsource and LOPAC collections to inhibit HCMV strain AD169 pp28
736 protein production in HFF cells was investigated. After exclusion of compounds
737 judged to be cytotoxic, each compound was assigned a z-score (the number of
738 standard deviations from the mean value of the screen) to describe the number of
739 cells expressing the HCMV antigen pp28. Thus, negative and positive z-scores
740 represented fewer or greater numbers of cells expressing pp28, respectively. A
741 plot of all z-scores is shown for each collection, where each data point represents
742 a single compound. List of compounds from each collection with their assigned z-
743 scores are shown in Tables S4-S6. The z-scores of RO-90-7501, PMEG and
744 Valaciclovir are indicated with red arrows. The structure of RO-90-7501 is also
745 shown.

746

747 **Fig 2. Structure of bisbenzimidazole compounds.** (A) The structure of Hoechst
748 33258 is shown. The binding of Hoechst 33258 to DNA via hydrogen bonds
749 between amine groups in Hoechst 33258 and oxygen and nitrogen atoms in
750 Adenine and Thymine nucleotides (40) is indicated with red dotted lines. (B) The
751 structure of RO-90-7501 is shown and the predicted binding of this compound to
752 DNA via hydrogen bonding is indicated in red dotted lines.

753

754 **Figure 3 Anti-HCMV activity of RO-90-7501 analogues.** HFF cells were infected
755 with HCMV strain AD169 (MOI 1) in the presence of the compounds indicated in

756 the figure (1 μ M) or the equivalent volume of DMSO. At 96 hours post infection
757 virus titre (plaque forming units/ml) from these infections was determined. The data
758 points from three independent experiments are shown. The columns and error bars
759 represent the mean and standard deviations, respectively, of those data points.
760 The structure of the bisbenzimidazole compounds examined are shown to the right of
761 the figure. Amine groups thought to be involved in DNA binding in each compound
762 are highlighted in red text. Terminal amine groups of the compounds are
763 highlighted in green boxes.

764

765 **Fig 4. Virus replication and toxicity in the presence of RO-90-7501 or**
766 **MRT00210423.** HFF cells were infected with HCMV strain (A) AD169 or (B)
767 Merlin(R1111) and then treated with the concentrations of RO-90-7501 or
768 MRT00210423 indicated in the figure or the corresponding volume of DMSO. Virus
769 production at 96 hours post infection is shown as the percentage of infectious virus
770 in the presence of RO-90-7501 or MRT00210423 compared to the appropriate
771 DMSO control. The titre of the viruses analyzed in these figures is shown in Figure
772 S2. (C and D) A high and low concentration of HFF cells (C and D, respectively,
773 see Materials and Methods) were treated for 96 hours with the concentrations of
774 RO-90-7501 or MRT00210423 indicated in the figure or the corresponding volume
775 of DMSO and then examined using an MTT assay. The data points and error bars
776 in each panel represent the mean of three independent experiments and the
777 standard deviation of those experiments, respectively. At some data points, the
778 error bars are too small to be represented on the figure.

779

780 **Fig 5. Association of RO-90-7501 and MRT00210423 with host cell chromatin.**

781 HFF cells were treated with decreasing concentrations (10, 1, 0.1 μ M, left to right
782 in the figure) of RO-90-7501 or MRT00210423 or the equivalent volume of DMSO
783 and examined by light microscopy. Brightfield (A-C, G-I, M-O) and UV emission
784 images (D-F, J-L, P-R, S-U) are shown. In Panels S-U images have been
785 manipulated using Photoshop to increase the brightness of the UV emission from
786 HFF cells treated with MRT00210423 (panels P-R).

787

788 **Fig. 6 Association of RO-90-7501 and MRT00210423 with plasmid DNA.**

789 (A) and (B) the number of putative compound binding sites in the sequence of
790 pUC19 and the HCMV AD169 genome, respectively. (C) RO-90-7501 or (D)
791 MRT00210423 was incorporated into agarose gels. Linear pUC19 plasmid
792 (2.6kbp) and a DNA molecular weight ladder were introduced into the gel via
793 electrophoresis and the gel was subjected to UV radiation. In both figures: Lane 1;
794 DNA molecular weight ladder, Lanes 2-onward; two-fold dilution series of 1 μ g
795 linear pUC19 plasmid. The position of pUC19 is indicated with an arrow to the right
796 of each figure. The position of the 3kbp marker in Lane 1 is indicated to the left of
797 each figure.

798

799 **Fig 7. Investigation of MRT00210423 analogues anti-HCMV activity and their**

800 **association with DNA.** (A) HFF were infected with HCMV strain AD169 (MOI 1)

801 in the presence of the compounds indicated in the figure (1 μ M) or an equivalent
802 volume of DMSO. At 96 hours post infection virus titre (plaque forming units/ml)
803 from these infections was determined. The data points from three independent
804 experiments are shown. The columns and error bars represent the mean and
805 standard deviations, respectively, of those data points. The structure of the
806 bisbenzimidazole compounds examined are shown to the right of the figure. The
807 methyl groups substituted for amine groups are highlighted in red in MRT00210426
808 and MRT00210427.

809

810 **Fig 8. Single molecule imaging of a quantum dot in the presence of RO-90-**
811 **7501 or MRT00210423.** A schematic of the experiment is shown in panel A. A
812 microscopy flow cell containing bacteriophage lambda DNA conjugated with a
813 quantum dot was prepared as described in the Materials and methods. Buffer
814 containing (B) a volume of DMSO equivalent to 75 μ M or either compound (C) 75
815 μ M RO-90-7501 or (D) 75 μ M MRT00210423 was flowed into the microscopy flow
816 cell and movement of the quantum dot was recorded using a total internal reflection
817 fluorescence microscope. Kymograph panels (B)-(D) show sequential images of
818 the quantum dot in buffer containing either DMSO, RO-90-7501 or MRT00210423
819 over time. The time frame of the images and the distance are represented with
820 horizontal and vertical bars, respectively, in each panel. The direction of the buffer
821 flowing into the microscopy cell is shown with an arrow. In (B) arrows are used to
822 shown the position of the quantum dot.

823

824 **Fig 9. Production of HCMV proteins, DNA and capsids in the presence of**
825 **bisbenzimidazole compounds.** (A) HFF cells were infected with HCMV strain AD169
826 and treated with the concentrations of RO-90-7501, MRT00210423 (both in 2-fold
827 dilution series starting at 10 μ M) or the corresponding volumes of DMSO. Cell
828 lysates were prepared for western blotting at 72 hours post infection. Western
829 blotting was used to detect viral (IE1/IE2, UL57 and pp28) and cellular (β -actin)
830 proteins in infected cells treated with either DMSO (lanes 2 and 5) or RO-90-7501
831 (lanes 3 and 6) or MRT00210423 (lanes 4 and 7). Uninfected cells were harvested
832 for analysis at the time of infection (lane 1). Proteins recognized by the antibodies
833 used are indicated to the right of each figure. The positions of molecular mass
834 markers (kDa) are indicated to the left of each figure. Blots for IE1/IE2 and UL57
835 or pp28 were performed on separate gels. (B) Viral DNA synthesis was determined
836 by quantitative real-time PCR analysis of DNA prepared from infected HFF cell
837 lysate (AD169, MOI 1, in the presence of 1 μ M or 10 μ M compound or the
838 equivalent volume of DMSO) prepared at the time points indicated in the figure.
839 The amount of viral DNA detected was represented as copies of the viral gene
840 *UL83* per copy of the cellular *adipsin* gene. The data points from three independent
841 experiments are shown. The columns and error bars represent the mean and
842 standard deviations, respectively, of those data points. Statistical significance was
843 assayed using an unpaired t test and two-tailed p values are shown in the figure.
844 The fold difference between the values of the mean data is also noted above the
845 figure.

846

847 **Fig. 10 Production of HCMV capsids in the presence of bisbenzimidazole**
848 **compounds.** Infected cells from three independent experiments (HFF cells
849 infected with AD169 (MOI 1) for 96 hours in the presence of 1 μ M or 10 μ M of
850 either compound, or the equivalent volume of DMSO), were combined and
851 prepared for analysis by electron microscopy. In each condition, the number of A,
852 B and C capsids in 10 nucleus profiles selected at random were counted. Only
853 nuclei where the entire area of the nuclei could be visualized were counted.

854

855

856

857

858 **References**

859

860 1. Griffiths PD. Burden of disease associated with human cytomegalovirus
861 and prospects for elimination by universal immunisation. *The Lancet infectious*
862 *diseases*. 2012;12(10):790-8. doi: 10.1016/S1473-3099(12)70197-4

863 2. Krause PR, Bialek SR, Boppana SB, Griffiths PD, Laughlin CA, Ljungman
864 P, et al. Priorities for CMV vaccine development. *Vaccine*. 2013;32(1):4-10. doi:
865 10.1016/j.vaccine.2013.09.042

866 3. Coen DM, Schaffer PA. Antiherpesvirus drugs: a promising spectrum of new
867 drugs and drug targets. *Nat Rev Drug Discov*. 2003;2(4):278-88. doi:
868 10.1038/nrd1065

869 4. Lischka P, Hewlett G, Wunberg T, Baumeister J, Paulsen D, Goldner T, et
870 al. In vitro and in vivo activities of the novel anticytomegalovirus compound
871 AIC246. *Antimicrobial agents and chemotherapy*. 2010;54(3):1290-7. doi:
872 10.1128/AAC.01596-09

873 5. Biron KK, Harvey RJ, Chamberlain SC, Good SS, Smith AA, 3rd, Davis MG,
874 et al. Potent and selective inhibition of human cytomegalovirus replication by
875 1263W94, a benzimidazole L-riboside with a unique mode of action. *Antimicrobial*
876 *agents and chemotherapy*. 2002;46(8):2365-72. doi: 10.1128/AAC.46.8.2365-
877 2372.2002

878 6. Goldner T, Hewlett G, Ettischer N, Ruebsamen-Schaeff H, Zimmermann H,
879 Lischka P. The novel anticytomegalovirus compound AIC246 (Letemovir) inhibits
880 human cytomegalovirus replication through a specific antiviral mechanism that

881 involves the viral terminase. *J Virol.* 2011;85(20):10884-93. doi:
882 10.1128/JVI.05265-11

883 7. Chou S. A third component of the human cytomegalovirus terminase
884 complex is involved in letermovir resistance. *Antiviral research.* 2017;148:1-4. doi:
885 10.1016/j.antiviral.2017.10.019

886 8. Cherrier L, Nasar A, Goodlet KJ, Nailor MD, Tokman S, Chou S. Emergence
887 of letermovir resistance in a lung transplant recipient with ganciclovir-resistant
888 cytomegalovirus infection. *American journal of transplantation : official journal of*
889 *the American Society of Transplantation and the American Society of Transplant*
890 *Surgeons.* 2018;18(12):3060-4. doi: 10.1111/ajt.15135

891 9. Chou S, Satterwhite LE, Ercolani RJ. New Locus of Drug Resistance in the
892 Human Cytomegalovirus UL56 Gene Revealed by In Vitro Exposure to Letermovir
893 and Ganciclovir. *Antimicrobial agents and chemotherapy.* 2018;62(9). doi:
894 10.1128/AAC.00922-18

895 10. Chou S. Rapid In Vitro Evolution of Human Cytomegalovirus UL56
896 Mutations That Confer Letermovir Resistance. *Antimicrobial agents and*
897 *chemotherapy.* 2015;59(10):6588-93. doi: 10.1128/AAC.01623-15

898 11. Chou S, Wechel LC, Marousek GI. Cytomegalovirus UL97 kinase mutations
899 that confer maribavir resistance. *The Journal of infectious diseases.*
900 2007;196(1):91-4. doi: 10.1086/518514

901 12. Papanicolaou GA, Silveira FP, Langston AA, Pereira MR, Avery RK, Uknis
902 M, et al. Maribavir for Refractory or Resistant Cytomegalovirus Infections in
903 Hematopoietic-cell or Solid-organ Transplant Recipients: A Randomized, Dose-

904 ranging, Double-blind, Phase 2 Study. Clin Infect Dis. 2019;68(8):1255-64. doi:
905 10.1093/cid/ciy706

906 13. Marty FM, Ljungman P, Papanicolaou GA, Winston DJ, Chemaly RF,
907 Strasfeld L, et al. Maribavir prophylaxis for prevention of cytomegalovirus disease
908 in recipients of allogeneic stem-cell transplants: a phase 3, double-blind, placebo-
909 controlled, randomised trial. The Lancet infectious diseases. 2011;11(4):284-92.
910 doi: 10.1016/S1473-3099(11)70024-X

911 14. Marty FM, Boeckh M. Maribavir and human cytomegalovirus-what
912 happened in the clinical trials and why might the drug have failed? Current opinion
913 in virology. 2011;1(6):555-62. doi: 10.1016/j.coviro.2011.10.011

914 15. Mocarski ES, Shenk T, Griffiths PD, Pass RF. Cytomegaloviruses In: Knipe
915 DM, Howley PM, editors. Fields Virology. 2. 6th ed. New York, NY: Lippincott,
916 Williams & Wilkins; 2015. p. 1960-2015.

917 16. Mercorelli B, Luganini A, Nannetti G, Tabarrini O, Palu G, Gribaudo G, et
918 al. Drug Repurposing Approach Identifies Inhibitors of the Prototypic Viral
919 Transcription Factor IE2 that Block Human Cytomegalovirus Replication. Cell
920 chemical biology. 2016;23(3):340-51. doi: 10.1016/j.chembiol.2015.12.012

921 17. Gardner TJ, Cohen T, Redmann V, Lau Z, Felsenfeld D, Tortorella D.
922 Development of a high-content screen for the identification of inhibitors directed
923 against the early steps of the cytomegalovirus infectious cycle. Antiviral research.
924 2015;113:49-61. doi: 10.1016/j.antiviral.2014.10.011

- 925 18. Nukui M, O'Connor CM, Murphy EA. The Natural Flavonoid Compound
926 Deguelin Inhibits HCMV Lytic Replication within Fibroblasts. *Viruses*. 2018;10(11).
927 doi: 10.3390/v10110614
- 928 19. Mukhopadhyay R, Roy S, Venkatadri R, Su YP, Ye W, Barnaeva E, et al.
929 Efficacy and Mechanism of Action of Low Dose Emetine against Human
930 Cytomegalovirus. *PLoS pathogens*. 2016;12(6):e1005717. doi:
931 10.1371/journal.ppat.1005717
- 932 20. Strang BL. RO0504985 is an inhibitor of CMGC kinase proteins and has
933 anti-human cytomegalovirus activity. *Antiviral research*. 2017;144:21-6. doi:
934 10.1016/j.antiviral.2017.05.004
- 935 21. Khan AS, Murray MJ, Ho CMK, Zuercher WJ, Reeves MB, Strang BL. High-
936 throughput screening of a GlaxoSmithKline protein kinase inhibitor set identifies
937 an inhibitor of human cytomegalovirus replication that prevents CREB and histone
938 H3 post-translational modification. *J Gen Virol*. 2017;98(4):754-68. doi:
939 10.1099/jgv.0.000713
- 940 22. Beelontally R, Wilkie GS, Lau B, Goodmaker CJ, Ho CMK, Swanson CM,
941 et al. Identification of compounds with anti-human cytomegalovirus activity that
942 inhibit production of IE2 proteins. *Antiviral research*. 2017;138:61-7. doi:
943 10.1016/j.antiviral.2016.12.006
- 944 23. Polachek WS, Moshrif HF, Franti M, Coen DM, Sreenu VB, Strang BL. High-
945 Throughput Small Interfering RNA Screening Identifies Phosphatidylinositol 3-
946 Kinase Class II Alpha as Important for Production of Human Cytomegalovirus
947 Virions. *J Virol*. 2016;90(18):8360-71. doi: 10.1128/JVI.01134-16

- 948 24. Birmingham A, Selfors LM, Forster T, Wrobel D, Kennedy CJ, Shanks E, et
949 al. Statistical methods for analysis of high-throughput RNA interference screens.
950 Nature methods. 2009;6(8):569-75. doi: 10.1038/nmeth.1351
- 951 25. Zhang JH, Chung TD, Oldenburg KR. A Simple Statistical Parameter for
952 Use in Evaluation and Validation of High Throughput Screening Assays. Journal
953 of biomolecular screening. 1999;4(2):67-73. doi: 10.1177/108705719900400206
- 954 26. Loregian A, Coen DM. Selective anti-cytomegalovirus compounds
955 discovered by screening for inhibitors of subunit interactions of the viral
956 polymerase. Chem Biol. 2006;13(2):191-200. doi:
957 10.1016/j.chembiol.2005.12.002
- 958 27. Kim H, Loparo JJ. Observing Bacterial Chromatin Protein-DNA Interactions
959 by Combining DNA Flow-Stretching with Single-Molecule Imaging. Methods Mol
960 Biol. 2018;1837:277-99. doi: 10.1007/978-1-4939-8675-0_15
- 961 28. Kim H, Loparo JJ. Multistep assembly of DNA condensation clusters by
962 SMC. Nature communications. 2016;7:10200. doi: 10.1038/ncomms10200
- 963 29. Edelstein AD, Tsuchida MA, Amodaj N, Pinkard H, Vale RD, Stuurman N.
964 Advanced methods of microscope control using muManager software. J Biol
965 Methods. 2014;1(2). doi: 10.14440/jbm.2014.36
- 966 30. Schneider CA, Rasband WS, Eliceiri KW. NIH Image to ImageJ: 25 years
967 of image analysis. Nature methods. 2012;9(7):671-5. doi: 10.1038/nmeth.2089
- 968 31. Strang BL, Stow ND. Circularization of the herpes simplex virus type 1
969 genome upon lytic infection. J Virol. 2005;79(19):12487-94. doi:
970 10.1128/JVI.79.19.12487-12494.2005

- 971 32. Strang BL, Bender BJ, Sharma M, Pesola JM, Sanders RL, Spector DH, et
972 al. A mutation deleting sequences encoding the amino terminus of human
973 cytomegalovirus UL84 impairs interaction with UL44 and capsid localization. *J*
974 *Virol.* 2012;86(20):11066-77. doi: 10.1128/JVI.01379-12
- 975 33. Strang BL, Boulant S, Kirchhausen T, Coen DM. Host Cell Nucleolin Is
976 Required To Maintain the Architecture of Human Cytomegalovirus Replication
977 Compartments. *Mbio.* 2012;3(1):301-11. doi: ARTN e00301-11
978 10.1128/mBio.00301-11
- 979 34. Kremer JR, Mastronarde DN, McIntosh JR. Computer visualization of three-
980 dimensional image data using IMOD. *Journal of structural biology.* 1996;116(1):71-
981 6. doi: 10.1006/jsbi.1996.0013
- 982 35. Wilkinson GW, Davison AJ, Tomasec P, Fielding CA, Aicheler R, Murrell I,
983 et al. Human cytomegalovirus: taking the strain. *Medical microbiology and*
984 *immunology.* 2015;204(3):273-84. doi: 10.1007/s00430-015-0411-4
- 985 36. Britt WJ, Jarvis M, Seo JY, Drummond D, Nelson J. Rapid genetic
986 engineering of human cytomegalovirus by using a lambda phage linear
987 recombination system: demonstration that pp28 (UL99) is essential for production
988 of infectious virus. *J Virol.* 2004;78(1):539-43. doi: 10.1128/jvi.78.1.539-543.2004
- 989 37. Depto AS, Stenberg RM. Functional analysis of the true late human
990 cytomegalovirus pp28 upstream promoter: cis-acting elements and viral trans-
991 acting proteins necessary for promoter activation. *J Virol.* 1992;66(5):3241-6. doi:
992 10.1128/JVI.66.5.3241-3246.1992

- 993 38. De Clercq E, Sakuma T, Baba M, Pauwels R, Balzarini J, Rosenberg I, et
994 al. Antiviral activity of phosphonylmethoxyalkyl derivatives of purine and
995 pyrimidines. *Antiviral research*. 1987;8(5-6):261-72. doi: 10.1016/s0166-
996 3542(87)80004-9
- 997 39. Elion GB. Mechanism of action and selectivity of acyclovir. *The American*
998 *journal of medicine*. 1982;73(1A):7-13. doi: 10.1016/0002-9343(82)90055-9
- 999 40. Teng MK, Usman N, Frederick CA, Wang AH. The molecular structure of
1000 the complex of Hoechst 33258 and the DNA dodecamer d(CGCGAATTCGCG).
1001 *Nucleic Acids Res*. 1988;16(6):2671-90. doi: 10.1093/nar/16.6.2671
- 1002 41. Yakimovich A, Huttunen M, Zehnder B, Coulter LJ, Gould V, Schneider C,
1003 et al. Inhibition of Poxvirus Gene Expression and Genome Replication by
1004 Bisbenzimidazole Derivatives. *J Virol*. 2017;91(18). doi: 10.1128/JVI.00838-17
- 1005 42. Olive PL, Chaplin DJ, Durand RE. Pharmacokinetics, binding and
1006 distribution of Hoechst 33342 in spheroids and murine tumours. *Br J Cancer*.
1007 1985;52(5):739-46. doi: 10.1038/bjc.1985.252
- 1008 43. Patel SR, Kvols LK, Rubin J, O'Connell MJ, Edmonson JH, Ames MM, et
1009 al. Phase I-II study of pibenzimol hydrochloride (NSC 322921) in advanced
1010 pancreatic carcinoma. *Invest New Drugs*. 1991;9(1):53-7. doi:
1011 10.1007/BF00194545
- 1012 44. Faulds D, Heel RC. Ganciclovir. A review of its antiviral activity,
1013 pharmacokinetic properties and therapeutic efficacy in cytomegalovirus infections.
1014 *Drugs*. 1990;39(4):597-638. doi: 10.2165/00003495-199039040-00008

- 1015 45. Harshman KD, Dervan PB. Molecular recognition of B-DNA by Hoechst
1016 33258. *Nucleic Acids Res.* 1985;13(13):4825-35. doi: 10.1093/nar/13.13.4825
- 1017 46. Hampshire AJ, Fox KR. The effects of local DNA sequence on the
1018 interaction of ligands with their preferred binding sites. *Biochimie.* 2008;90(7):988-
1019 98. doi: 10.1016/j.biochi.2008.01.001
- 1020 47. Saito M, Kobayashi M, Iwabuchi S, Morita Y, Takamura Y, Tamiya E. DNA
1021 condensation monitoring after interaction with hoechst 33258 by atomic force
1022 microscopy and fluorescence spectroscopy. *J Biochem.* 2004;136(6):813-23. doi:
1023 10.1093/jb/mvh191
- 1024 48. Strang BL, Boulant S, Chang L, Knipe DM, Kirchhausen T, Coen DM.
1025 Human Cytomegalovirus UL44 Concentrates at the Periphery of Replication
1026 Compartments, the Site of Viral DNA Synthesis. *Journal of Virology.*
1027 2012;86(4):2089-95. doi: 10.1128/Jvi.06720-11
- 1028 49. Guo F, Mead J, Aliya N, Wang L, Cuconati A, Wei L, et al. RO 90-7501
1029 enhances TLR3 and RLR agonist induced antiviral response. *PloS one.*
1030 2012;7(10):e42583. doi: 10.1371/journal.pone.0042583
- 1031 50. Bathini Y, Rao KE, Shea RG, Lown JW. Molecular recognition between
1032 ligands and nucleic acids: novel pyridine- and benzoxazole-containing agents
1033 related to Hoechst 33258 that exhibit altered DNA sequence specificity deduced
1034 from footprinting analysis and spectroscopic studies. *Chem Res Toxicol.*
1035 1990;3(3):268-80. doi: 10.1021/tx00015a013
- 1036 51. Guan LL, Zhao R, Lown JW. Enhanced DNA alkylation activities of Hoechst
1037 33258 analogues designed for bioreductive activation. *Biochemical and*

1038 biophysical research communications. 1997;231(1):94-8. doi:
1039 10.1006/bbrc.1996.5908

1040 52. Gupta R, Wang H, Huang L, Lown JW. Design, synthesis, DNA sequence
1041 preferential alkylation and biological evaluation of N-mustard derivatives of
1042 Hoechst 33258 analogues. *Anticancer Drug Des.* 1995;10(1):25-41. doi:
1043 53. Kumar S, Yadagiri B, Zimmermann J, Pon RT, Lown JW. Sequence specific
1044 molecular recognition and binding by a GC recognizing Hoechst 33258 analogue
1045 to the decadeoxyribonucleotide d-[CATGGCCATG]₂: structural and dynamic
1046 aspects deduced from high field ¹H-NMR studies. *J Biomol Struct Dyn.*
1047 1990;8(2):331-57. doi: 10.1080/07391102.1990.10507809

1048 54. Rao KE, Lown JW. Molecular recognition between ligands and nucleic
1049 acids: DNA binding characteristics of analogues of Hoechst 33258 designed to
1050 exhibit altered base and sequence recognition. *Chem Res Toxicol.* 1991;4(6):661-
1051 9. doi: 10.1021/tx00024a011

1052 55. Singh MP, Joseph T, Kumar S, Bathini Y, Lown JW. Synthesis and
1053 sequence-specific DNA binding of a topoisomerase inhibitory analog of Hoechst
1054 33258 designed for altered base and sequence recognition. *Chem Res Toxicol.*
1055 1992;5(5):597-607. doi: 10.1021/tx00029a003
1056
1057

1058

1059

1060

1061

Table 1. Compounds assigned low z-scores in the screening assay.

1062

Compound	ChEMBL ID	Library	z-score
AM-251	CHEMBL285932	NIH Clinical Collection	-2.1
Ancitabine HCl	CHEMBL1412614	LOPAC	-3.0
Aurintricarboxylic acid	CHEMBL275938	LOPAC	-3.6
S-(p-Azidophenacyl) glutathione	-	LOPAC	-2.1
Carboplatin	CHEMBL1351	Microsource	-5.1
Cetirizine HCl	CHEMBL1000	Microsource	-2.1
Chloroxylenol	CHEMBL398440	Microsource	-2.1
Clonazepam	CHEMBL452	Microsource	-2.2
Clopidol	CHEMBL446918	Microsource	-2.1
Dibenzothiophene	CHEMBL219828	Microsource	-2.0
Floxuridine	CHEMBL917	NIH Clinical Collection	-3.5
Fludarabine	CHEMBL1568	NIH Clinical Collection	-3.2
Hexachlorophene	CHEMBL496	NIH Clinical Collection	-4.9
Hexylresorcinol	CHEMBL443605	Microsource	-2.0
Lisinopril	CHEMBL1237	Microsource	-2.1
Methotrexate	CHEMBL426	Microsource	-2.9
PMEG	CHEMBL20283	LOPAC	-5.4
Pyrimethamine	CHEMBL36	Microsource	-2.1
Raltitrexed	CHEMBL225071	NIH Clinical Collection	-3.0
Ranolazine	CHEMBL1404	Microsource	-2.2
Rifaximin	CHEMBL1617	Microsource	-2.3
RO-90-7501	-	LOPAC	-3.8
Salicylanilide	CHEMBL82970	Microsource	-2.0
Tamoxifen	CHEMBL83	Microsource	-2.5
Tenoxicam	CHEMBL302795	Microsource	-2.6
Unknown	-	NIH Clinical Collection	-2.4
Xylometazoline HCl	CHEMBL312448	Microsource	-2.1

1063

z-score (-2.0)-(-2.9) (-3.0)-(-3.9) (-4.0)-(-4.9) (-5.0)-(-5.9)

1064

1065

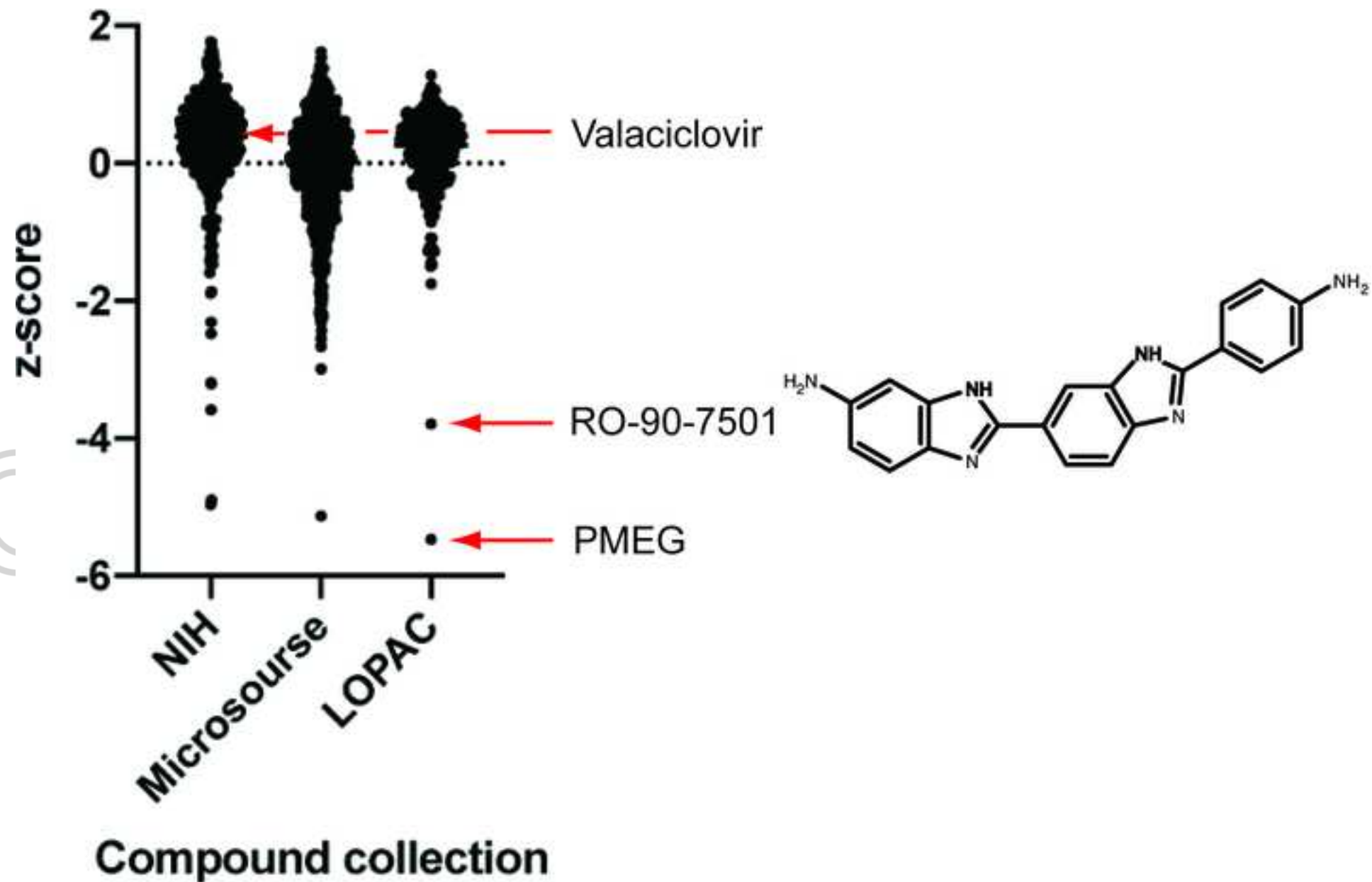


Figure 1

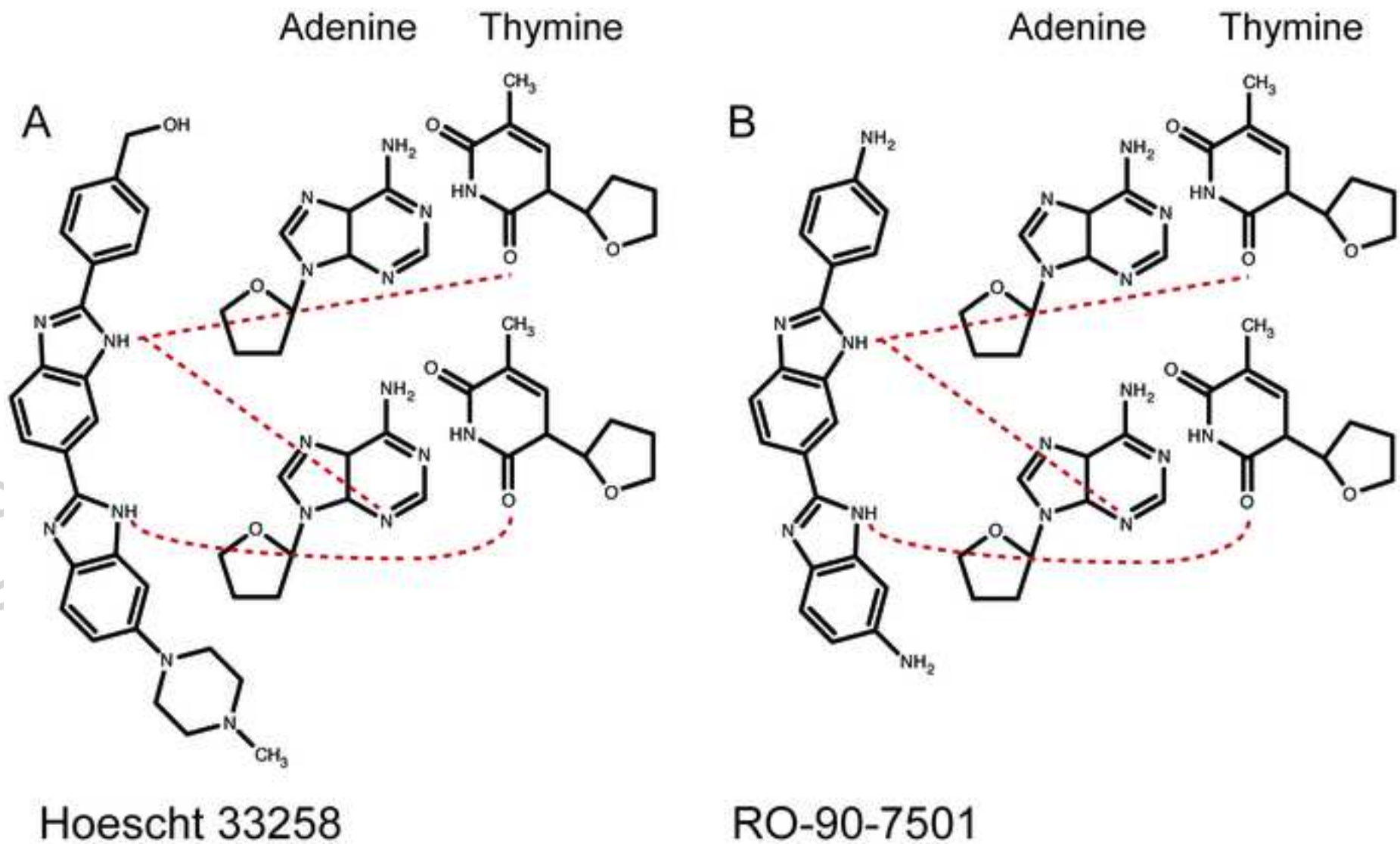


Figure 2

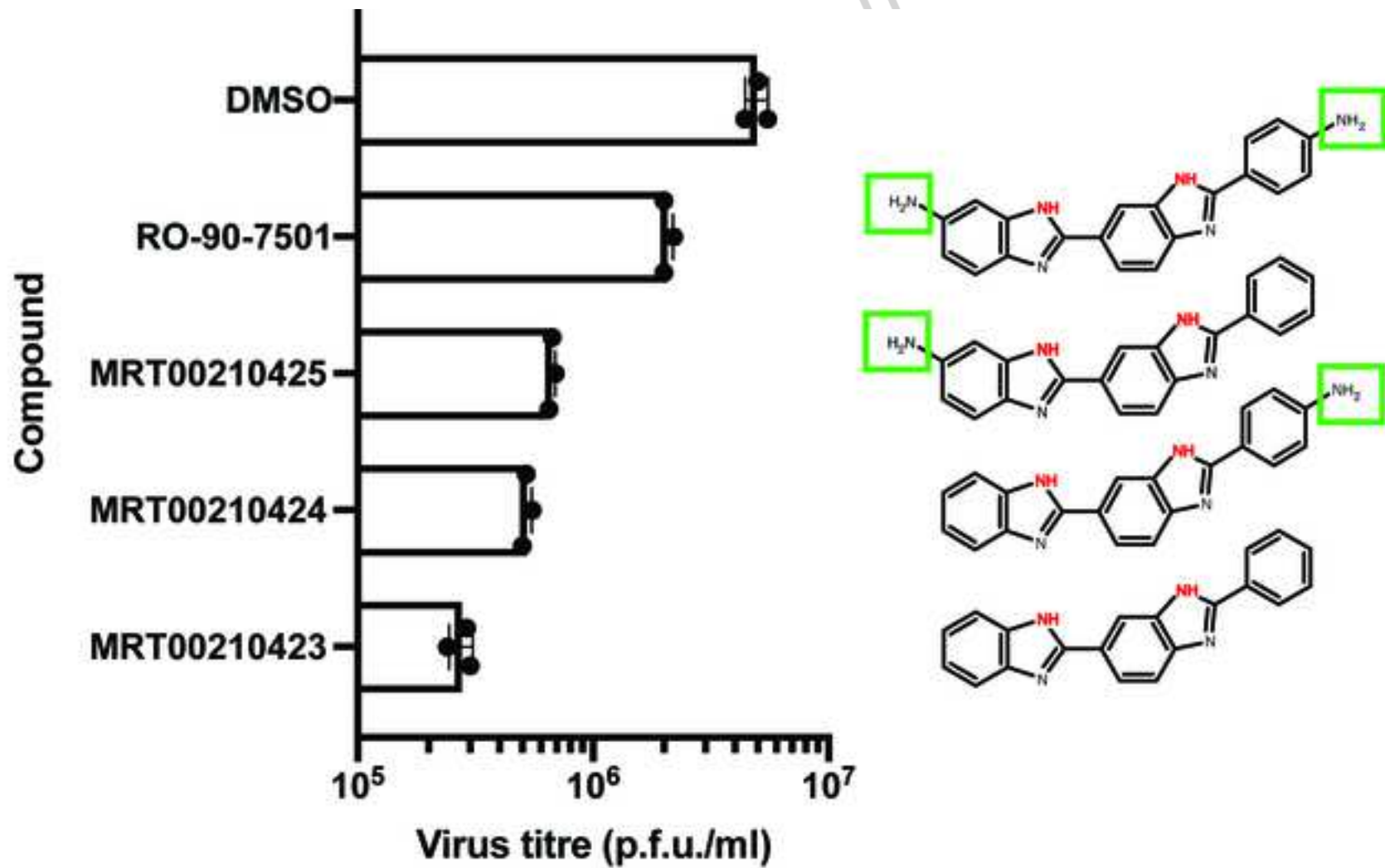


Figure 3

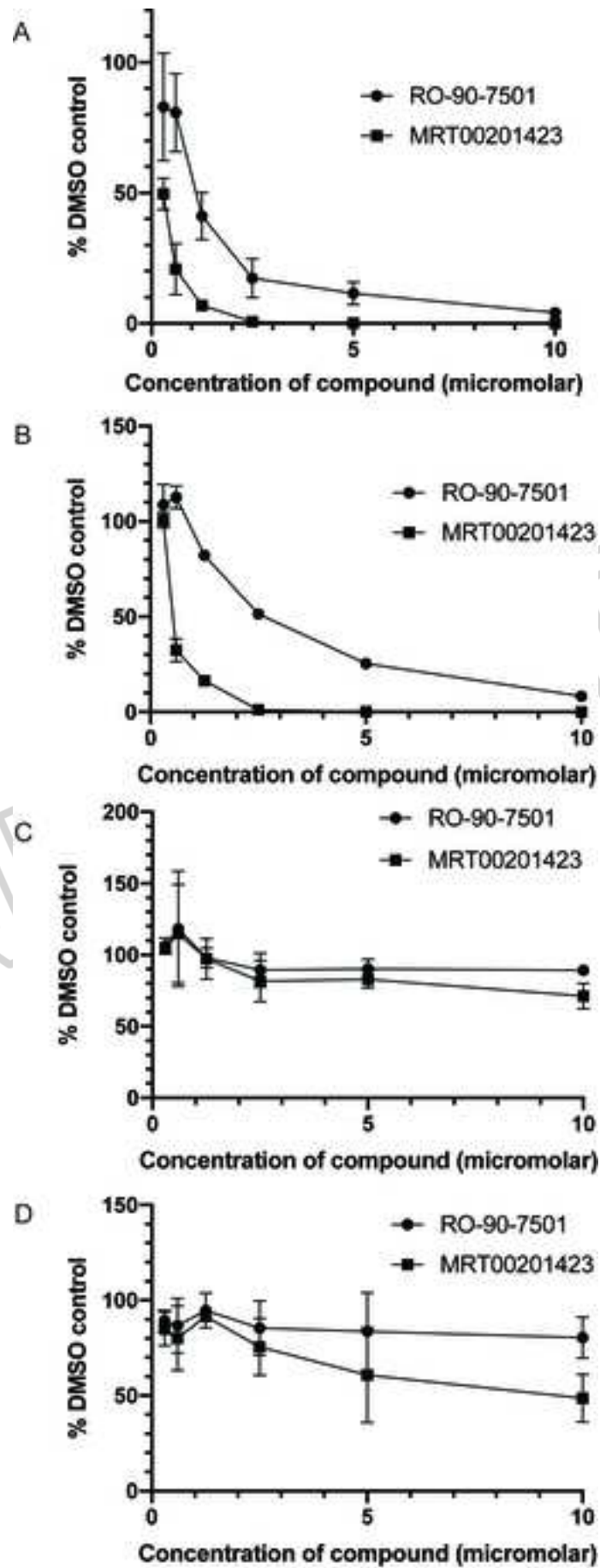


Figure 4

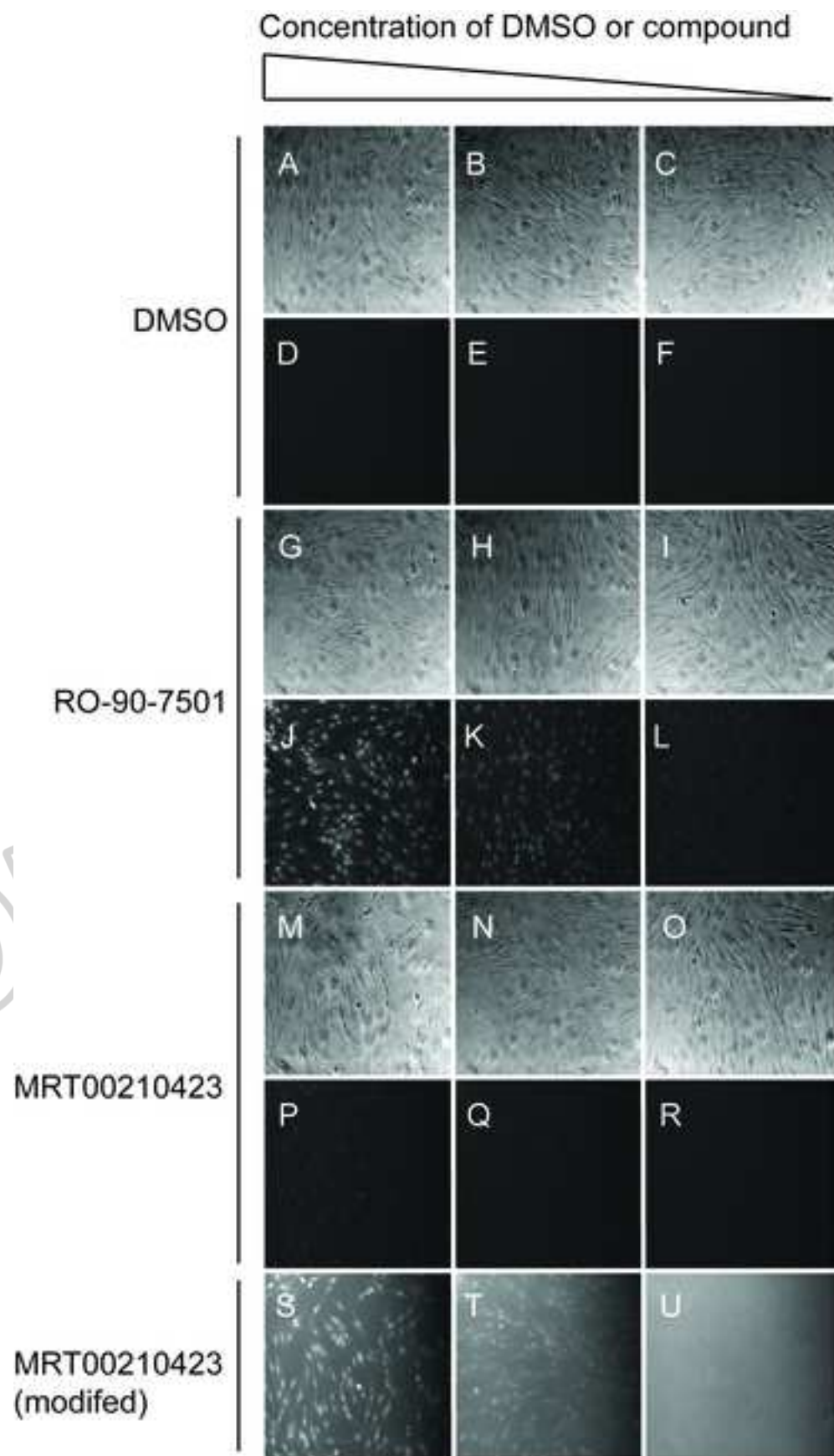


Figure 5

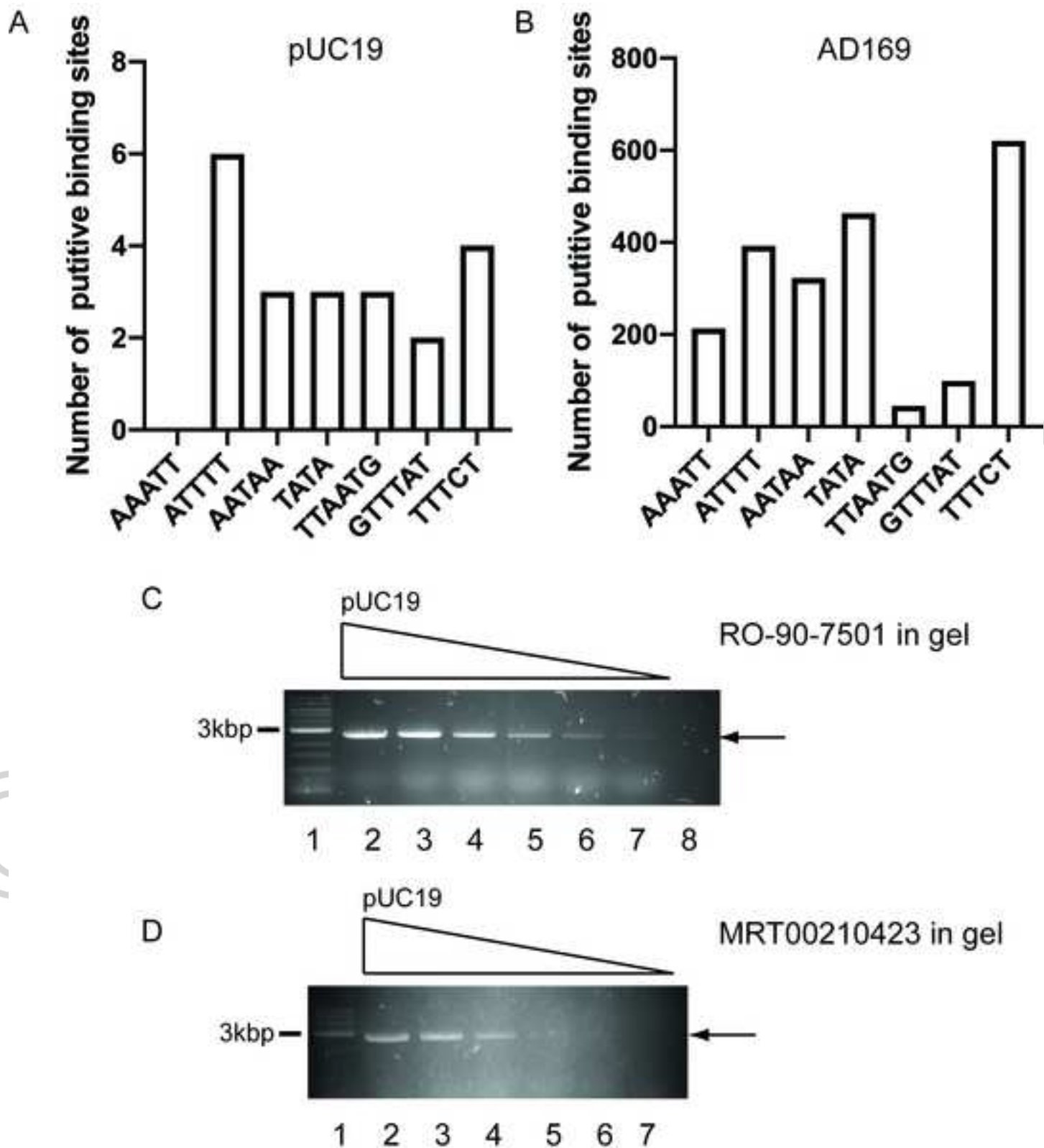


Figure 6

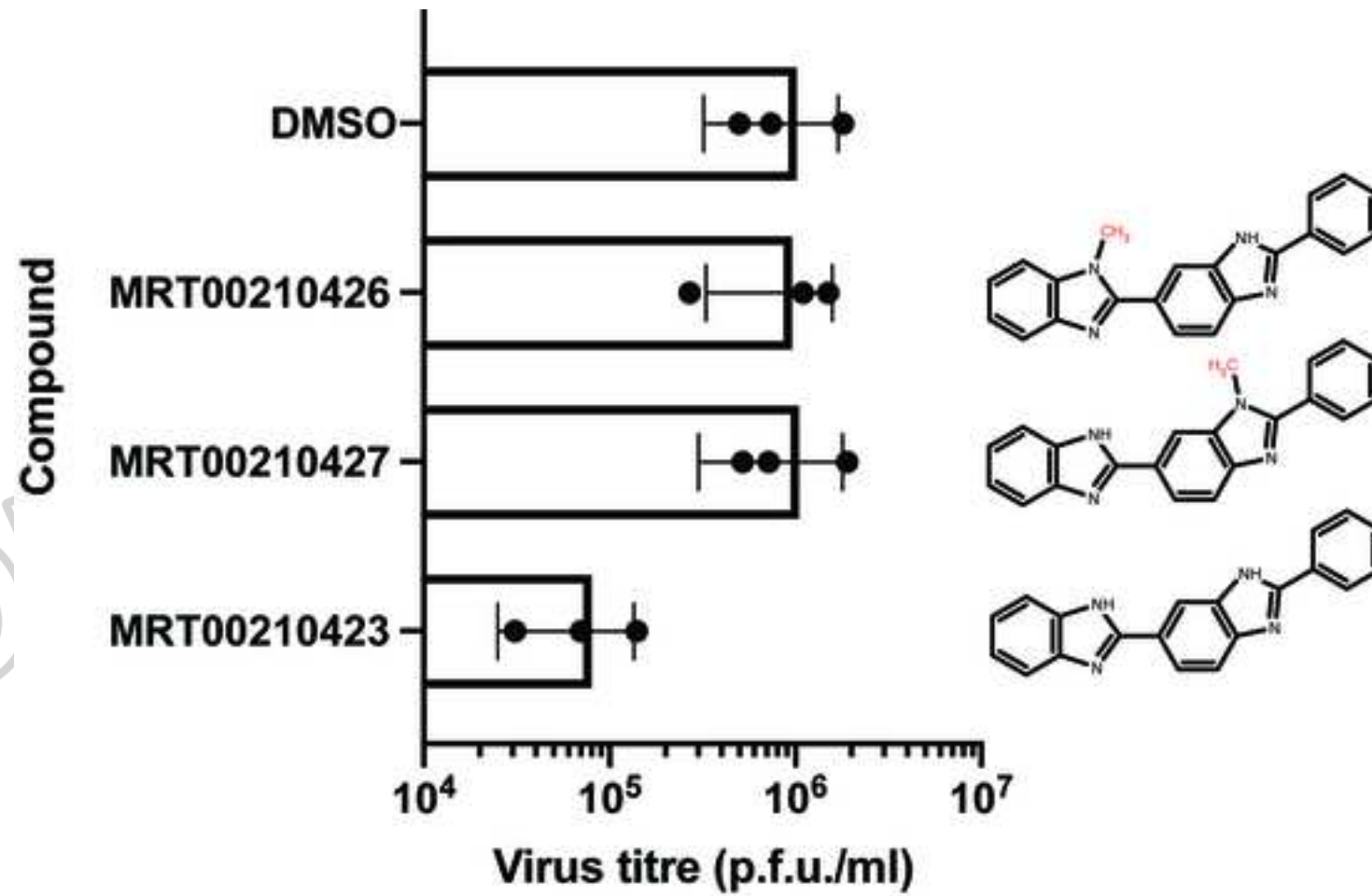


Figure 7

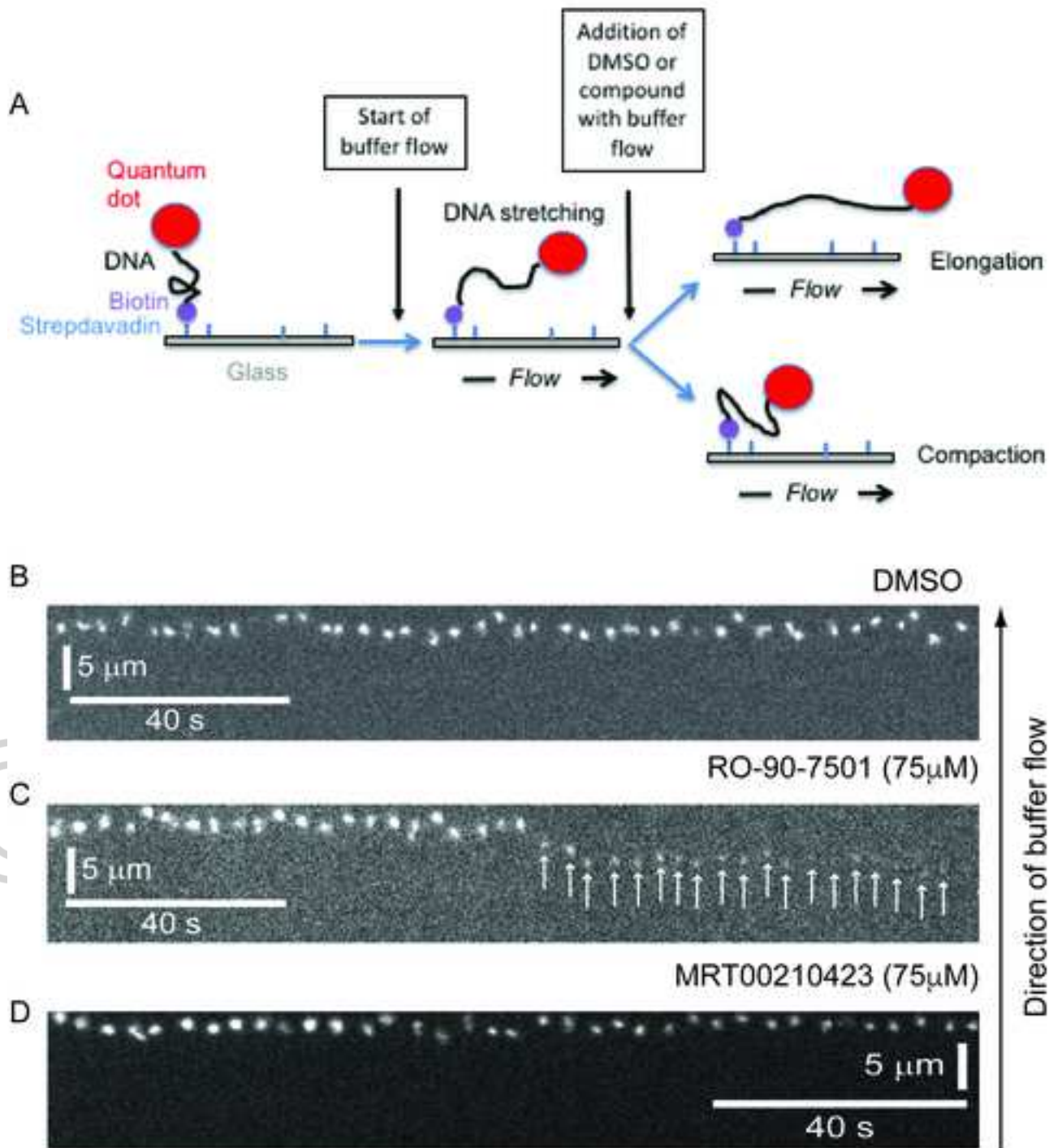


Figure 8

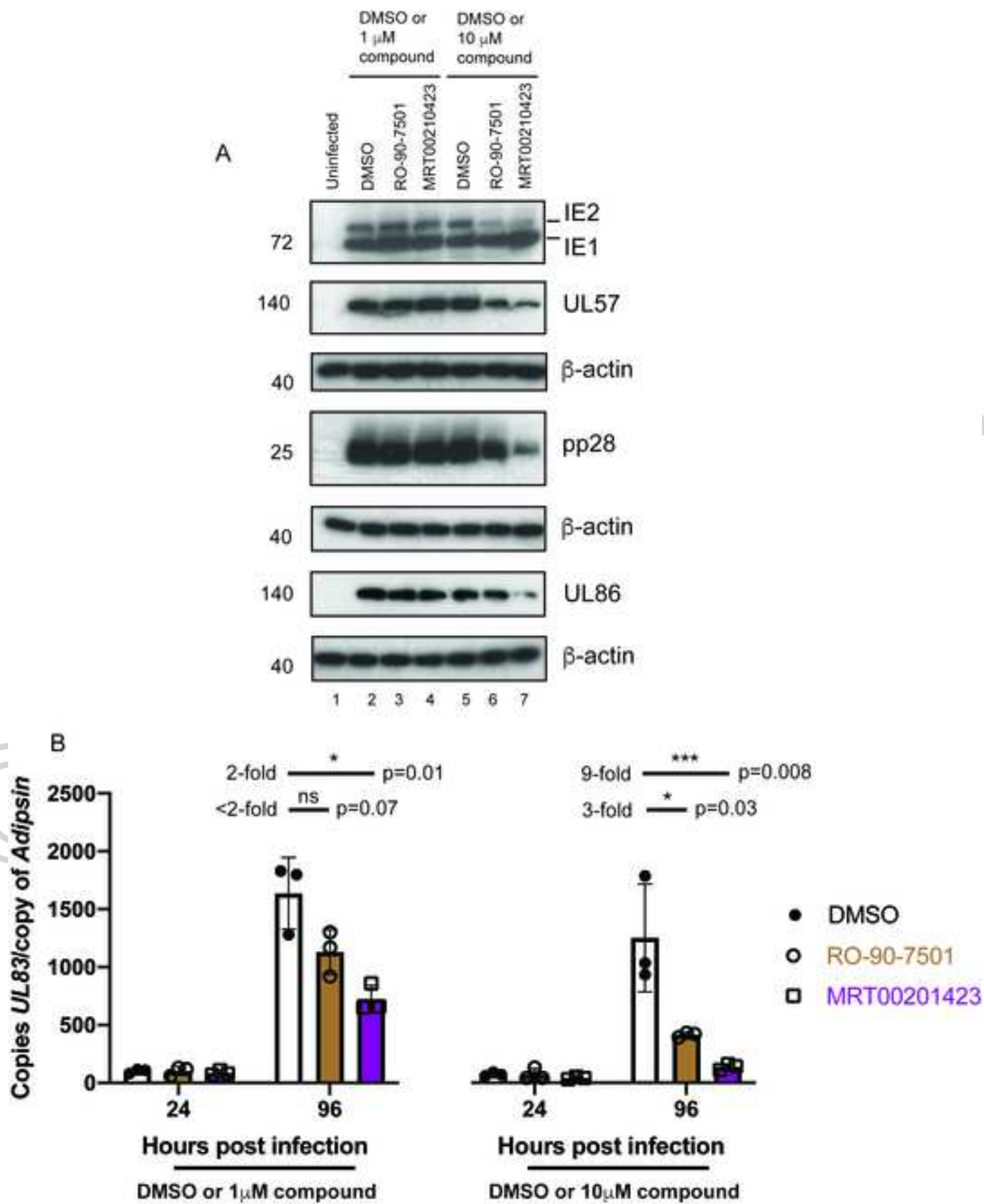


Figure 9

PREPRINT

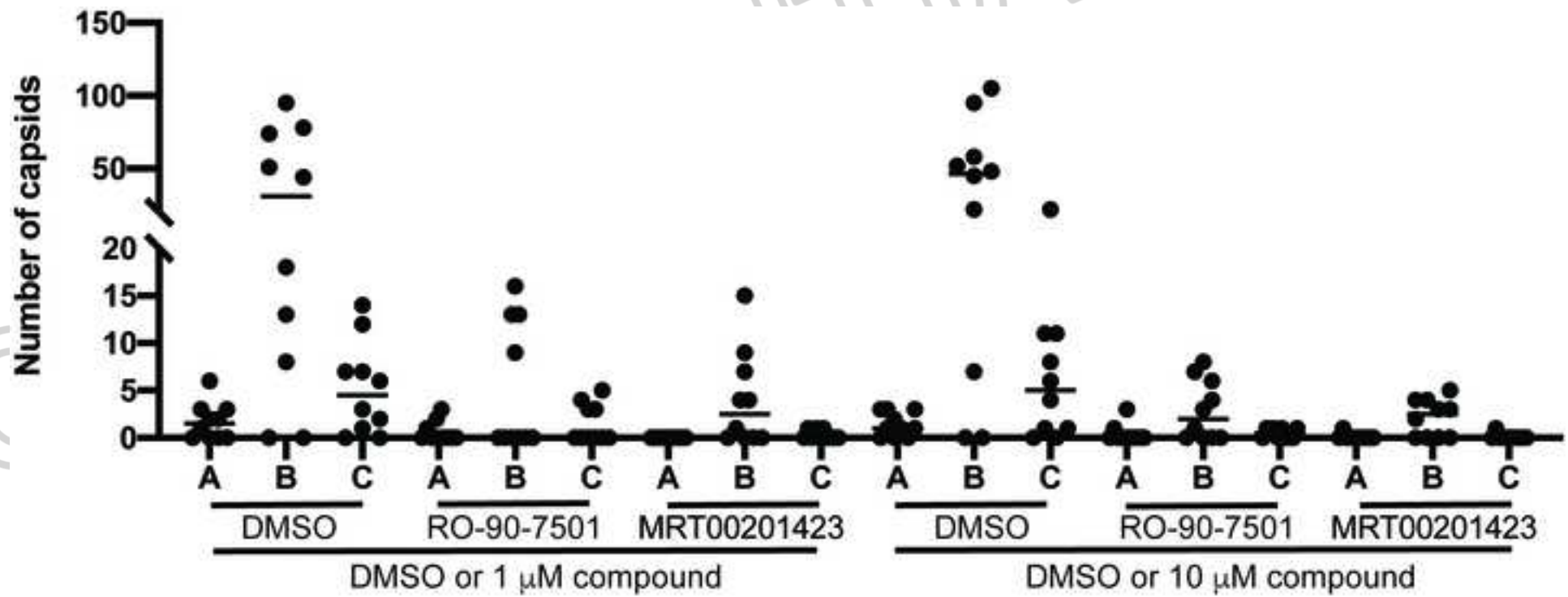


Figure 10

1 **Identification and characterization of bisbenzimidazole compounds that inhibit human**
2 **cytomegalovirus replication**

3 Nicole Falci Finardi, HyeongJun Kim, Lee Z Hernandez, Matthew RG Russell, Catherine M-
4 K Ho, Vattipally B Sreenu, Hannah A Wenham, Andy Merritt, & Blair L Strang

5

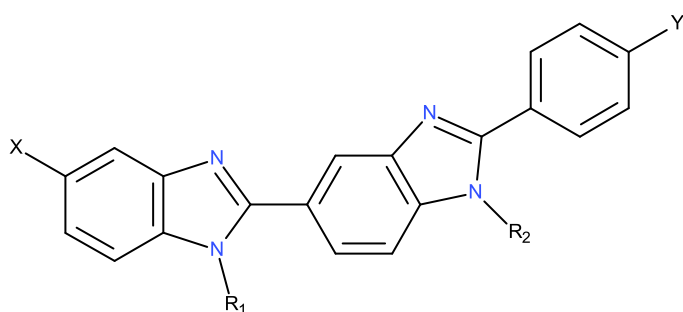
6 **Supplementary Figure 1 Synthesis of MRT00210 compounds**

7 In order to explore the importance of the various NH functionalities in RO-90-7510 a total of 5
8 compounds were designed and synthesised by LifeArc (see below).

9 Three these compounds explored the relative importance of the pendant NH₂ groups of RO-
10 90-7510; compound 423 had both amino groups replaced by hydrogens, compound 424
11 retained the amino group on the phenyl ring whilst the other NH₂ was replaced with H, and
12 compound 425 retained the amino group on the terminal benzimidazole portion but had no
13 NH₂ on the phenyl ring.

14 The other 2 compounds explored the importance of the benzimidazole NH. Based on the
15 unsubstituted core compound 423, compound 426 had the terminal benzimidazole NH
16 methylated whilst compound 427 had the central benzimidazole NH methylated.

17 A summary schema of the 5 compounds is shown below:



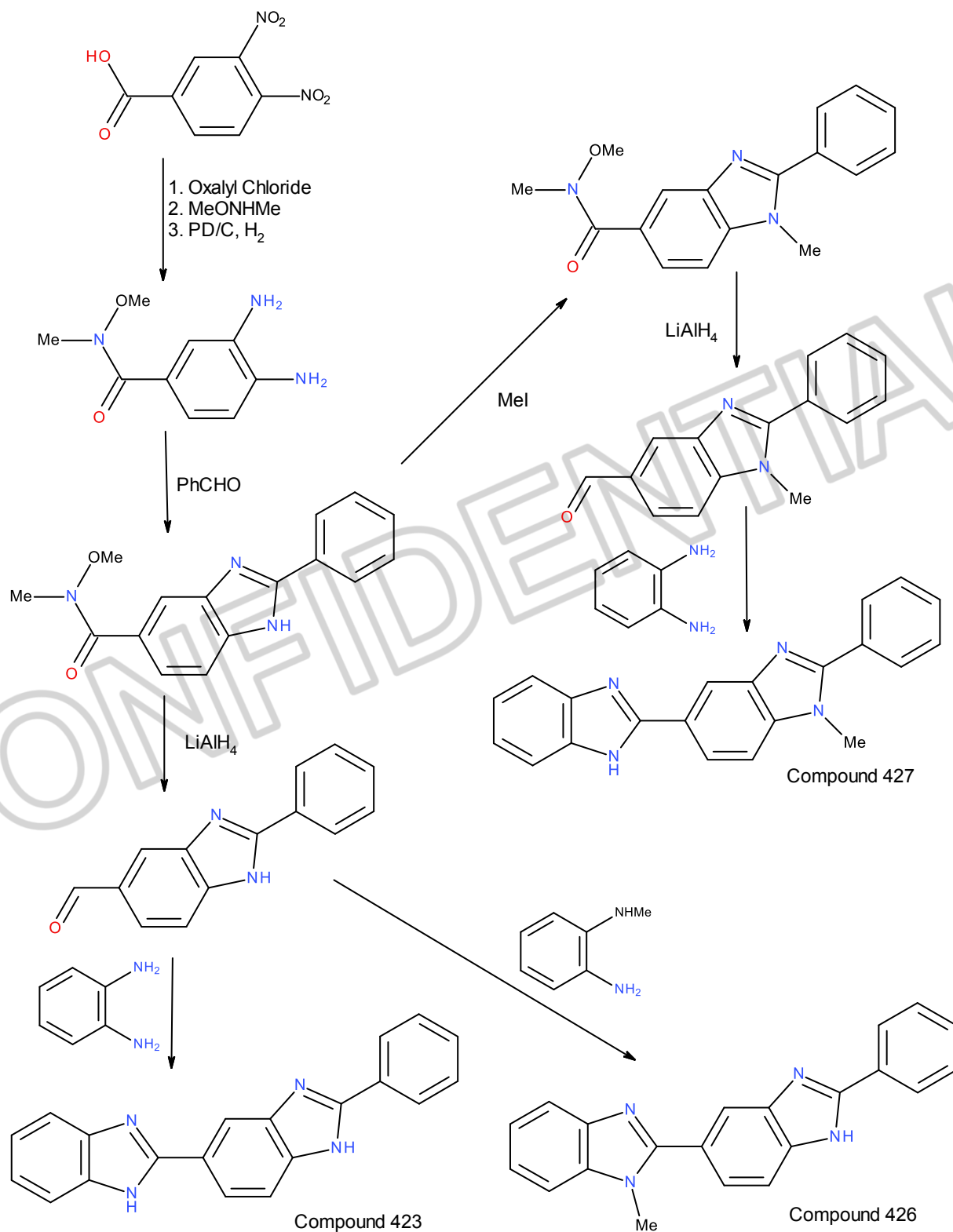
	X	Y	R ₁	R ₂
423	H	H	H	H
424	H	NH ₂	H	H
425	NH ₂	H	H	H
426	H	H	Me	H
427	H	H	H	Me

18

19

20

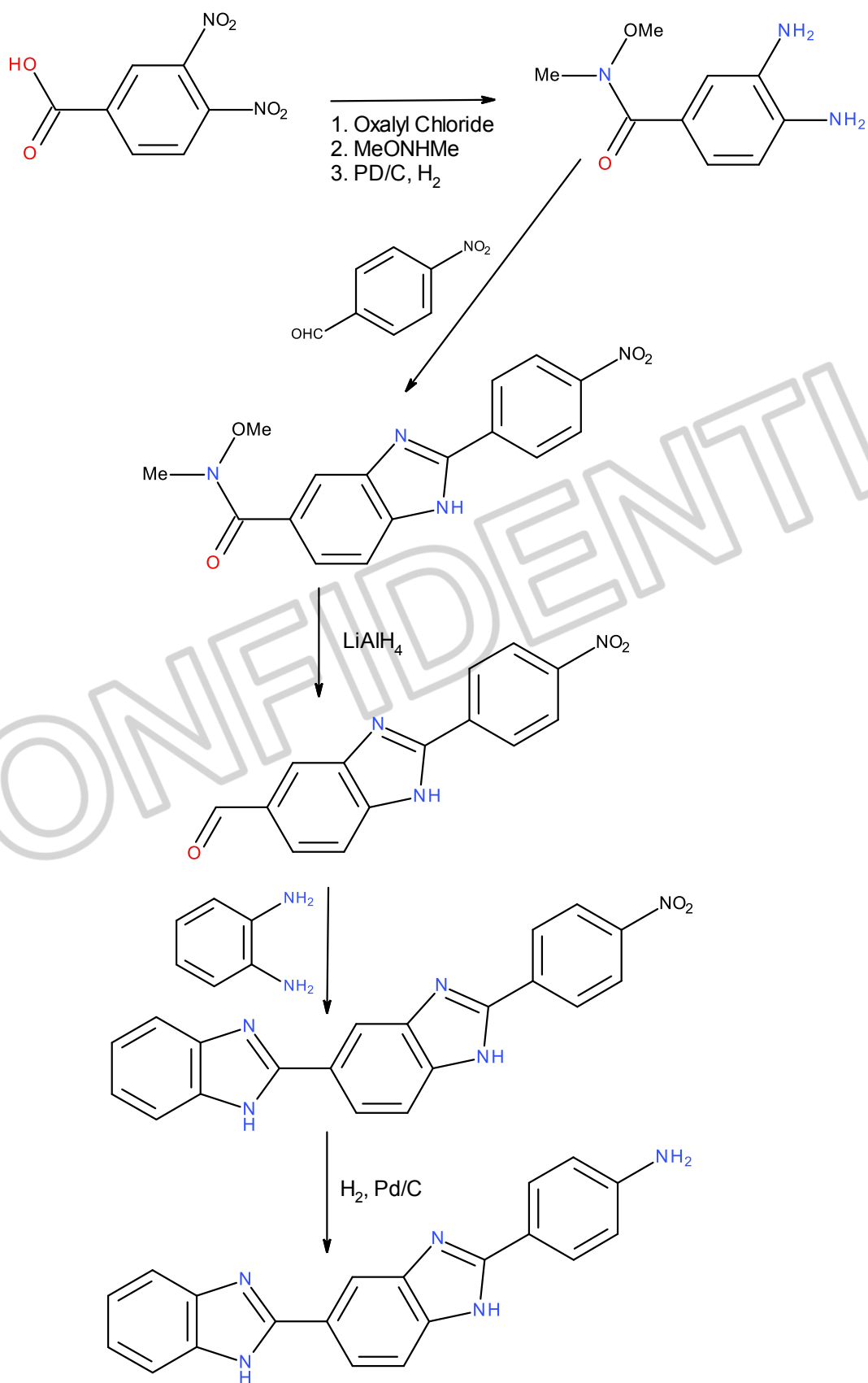
21 Syntheses of compounds 423, 426 and 427:



22

23

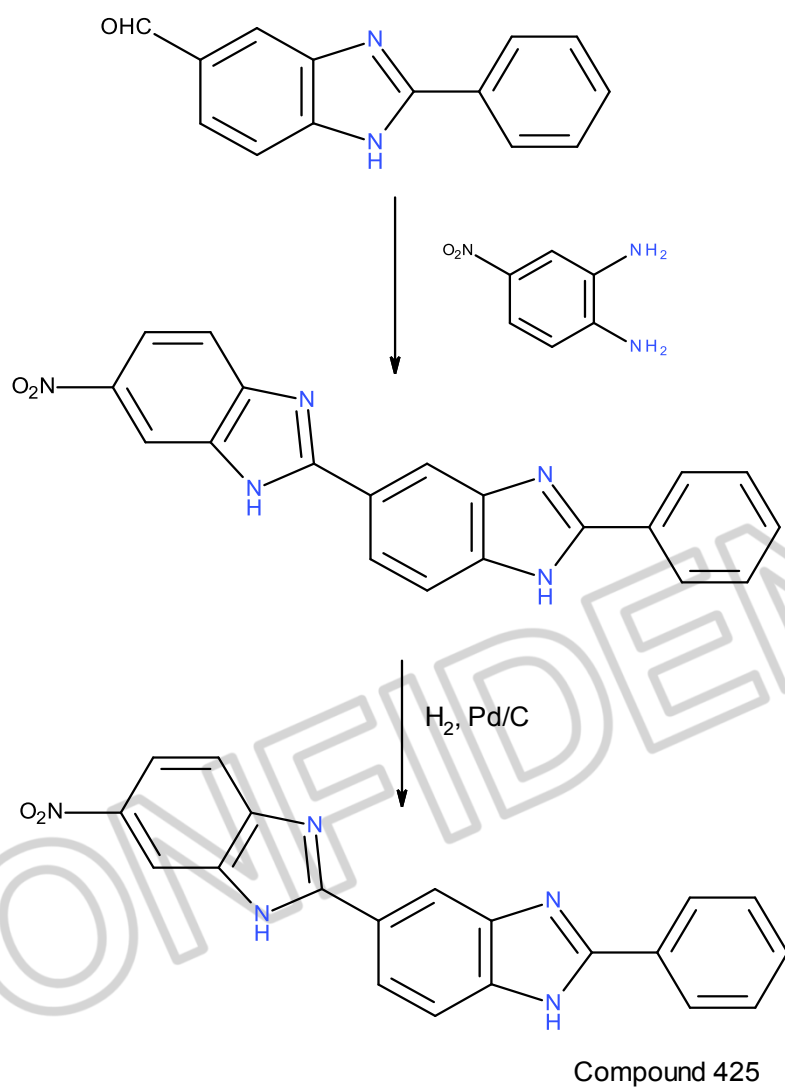
24 Synthesis of compound 424:



25

Compound 424

26 Synthesis of compound 425:



27

28

29

30

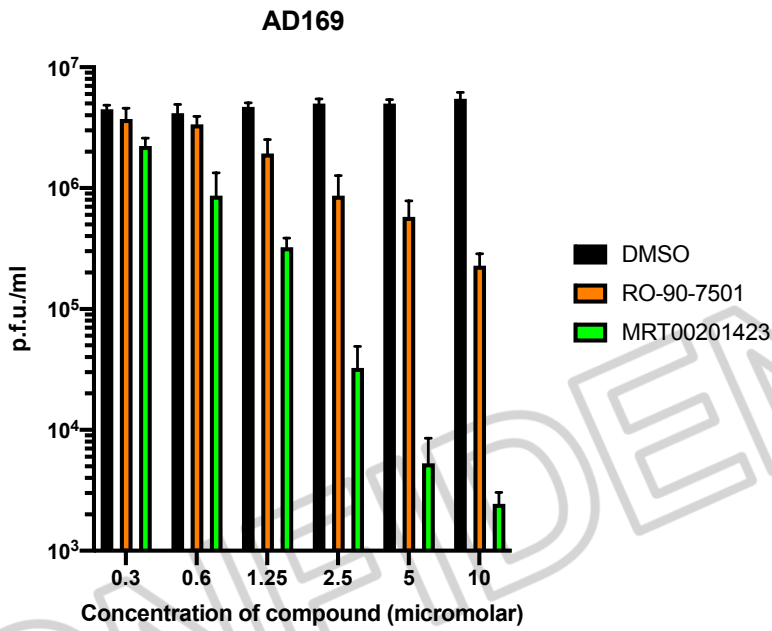
31

32

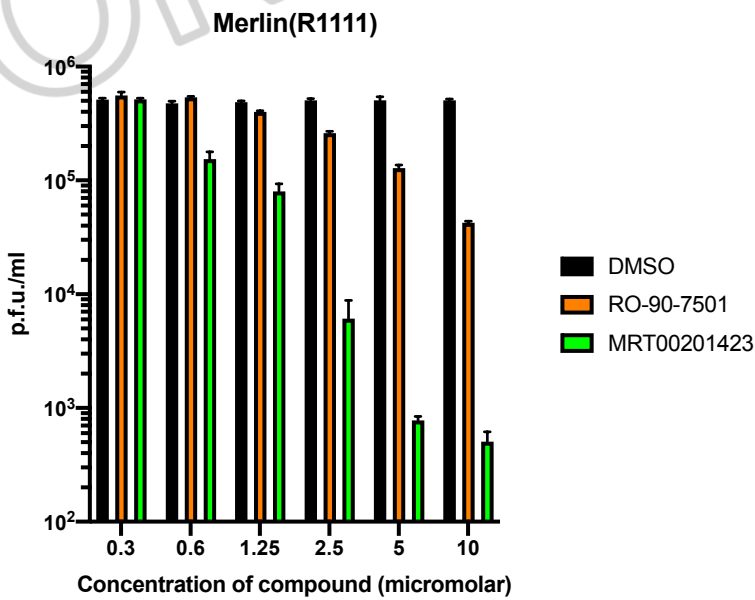
33

34 **Supplementary Figure 2 Titre of virus replication in the presence of bisbenzimidazole**
35 **compounds.** The titre of (A) AD169 and (B) Merlin(R1111) viruses from which the drug
36 susceptibility data in Figures 4A and 4B, respectively, was derived.

37 A



38 B

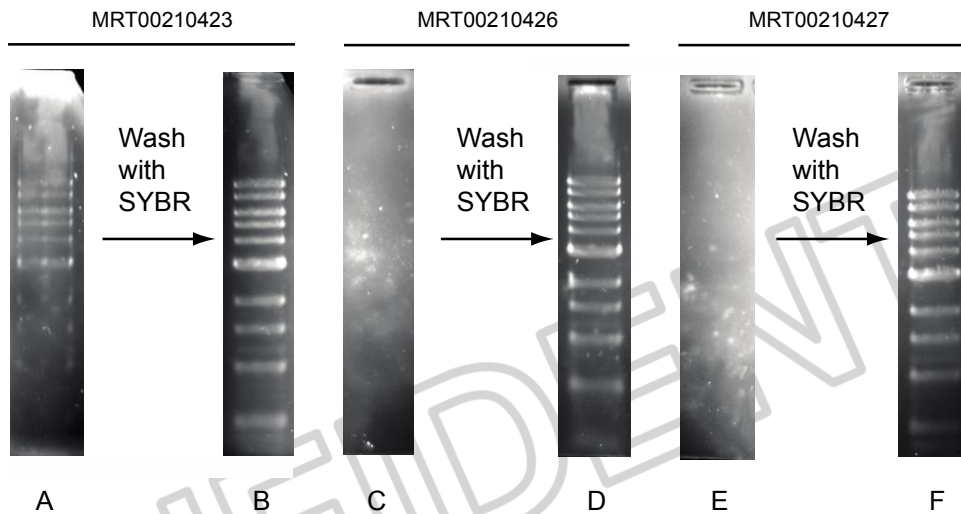


39

40

41

42 **Supplementary Figure 3 Investigation of MRT00210423 analogues association with**
43 **DNA.** A molecular weight DNA marker was introduced into agarose gels containing either (A)
44 MRT00210423, (C) MRT00210426 or (E) MRT00210427 using electrophoresis, which were
45 then exposed to UV light and photographed. Gels were then washed in SYBR, exposed to UV
46 light and photographed (panels (B), (D) and (F)).



47
48

CONFIDENTIAL

[Click here to access/download](#)

Supplementary Material - Excel file
S1-S8 file revised.xlsx

